Electronic Supplementary Material (ESI) for Journal of Materials Chemistry C.
This journal is © The Royal Society of Chemistry 2022

Electronic Supplementary Information

Observation of helical self-assembly in cyclic triphosphazene-based columnar liquid crystals bearing chiral mesogenic units

Shruti Rani,[a] Vidhika Punjani,[a] Santosh Prasad Gupta,[b] Madhu Babu Kanakala,[c] C. V. Yelamaggad*[c] and Santanu Kumar Pal*[a]

[a]*Department of Chemical Sciences, Indian Institute of Science Education and Research (IISER) Mohali, Punjab 140306, India*

[b]*Department of Physics, Patna University, Patna-800005, India*

[c]*Centre for Nano and Soft Matter Sciences, Bengaluru 560013, India*

E-mail: skpal@iisermohali.ac.in; santanupal.20@gmail.com; yelamaggad@gmail.com

Experimental Section

a) Materials and reagents. Commercially available chemicals were used in p.a. quality as obtained from the suppliers. Bromoalkanoic acids, 4-nitrophenol, 4-hydroxyaldehyde, potassium iodide (KI), potassium bromide (KBr), potassium carbonate (K_2CO_3), hexachlorocyclotriphosphazene, *N*,*N'*-dicyclohexylcarbodiimide (DCC), 4-dimethylaminopyridine (DMAP) were purchased from Sigma-Aldrich whereas cholesterol was procured from HiMedia. Tetrahydrofuran (THF), dichloromethane (DCM), acetonitrile (ACN) and 2-butanone were procured from Merck. Column chromatographic separations were performed on silica gel (100-200) and neutral alumina. Thin layer chromatography (TLC) was performed on alumina sheets precoated with silica gel (Merck, Kieselgel 60, F254).

b) Instrumentation

Structural characterization. ^{1}H NMR (400 MHz) and ^{13}C NMR (100 MHz) spectra in $CDCl_3$ were recorded at room temperature using Bruker Biospin Switzerland Avance-iii 400 MHz spectrometer. Tetramethylsilane (TMS) was used as an internal standard. The detailed specifications of instruments used for structural characterization are similar as mentioned in our previous papers.[1-4]

Fourier-Transform Infrared (FTIR) Spectroscopy: Fourier-transform infrared (FTIR) spectra of the compounds in KBr pellet under nitrogen atmosphere were recorded on Perkin-Elmer Spectrum Two in the range of 400 to 4000 cm^{-1}.

Polarised Optical Microscopy (POM): Textural observations of the mesophase were performed with Nikon Eclipse LV100POL polarising microscope provided with a Linkam heating stage (LTS 420). All images were captured using a Q-imaging camera.

Differential Scanning Calorimetry (DSC) Study: The transition temperatures and associated enthalpy values were determined using a differential scanning calorimeter (Perkin Elmer DSC 8000 coupled to a controlled liquid nitrogen accessory (CLN_2)) which was operated at a scanning rate of 10 °C min^{-1} during both heating and cooling cycles.

Thermogravimetric Analysis (TGA): Thermogravimetric analysis (TGA) was carried out on a Shimadzu DTG-60 instrument under N_2 atmosphere with a heating rate of 5 ºC min^{-1}.

X-ray Diffraction (XRD) Studies: Small-angle and wide-angle X-ray diffraction (XRD) was carried out using CuKα (λ = 1.54 Å) radiation from a source (GeniX 3D, Xenocs) operating at 50 kV and 0.6 mA. The diffraction patterns were collected on a two-module Pilatus detector.

UV-vis Measurements: The UV-vis-NIR spectrophotometer from Agilent Technologies, Cary 5000 was used for recording UV-vis spectra of the micromolar solutions.

Fluorescence Spectroscopy: Fluorescence measurements were performed using a Hitachi F7000 spectrophotometer (Luma 40) from Quantum Northwest.

Circular Dichroism (CD) Spectroscopy: Circular Dichroism (CD) spectra of the samples (thin films) were recorded at ~ 22 ℃ under the nitrogen atmosphere on a J-820 spectropolarimeter (JASCO Ltd., Tokyo, Japan) equipped with a programmable hot stage (Mettler Toledo FP90). Newly procured rectangular quartz plates of dimensions 2 cm x 2 cm and 2 mm thickness were used for the cell fabrication.

Synthesis and characterization

Scheme S1. Synthetic scheme of the target compounds

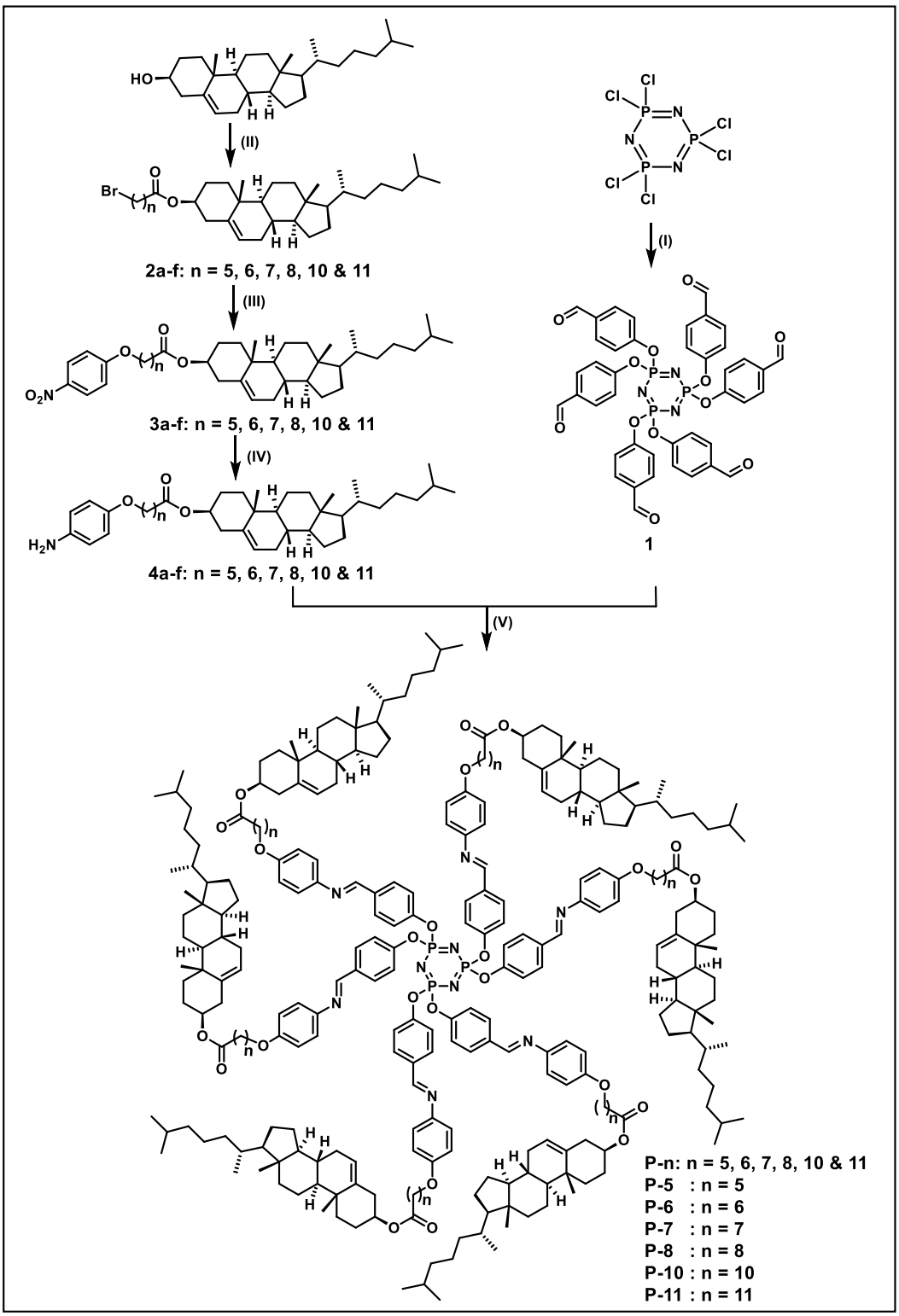

Reagents and conditions: (I) 4-Hydroxybenzaldehyde, K_2CO_3, THF, 70 °C, 48 h, 60 %; (II) DCC, DMAP, dry DCM, 60 °C, 12 h, (Yield = 75 - 78 %); (III) 4-nitrophenol, K_2CO_3, butanone, KI, 90 °C, 24 h, (Yield = 85 - 90 %); (IV) H_2, 10 % Pd/C, THF, RT, 48 h, (Quantitative Yield); (V) dry THF, 60 °C, 24 h (Yield = 35 - 40 %).

Synthesis of compound 1:

Hexachlorocyclotriphosphazene (600 mg, 1 equiv.) and potassium carbonate (3 g, 12 equiv.) was dissolved in dry THF (50 mL) under a nitrogen atmosphere with continuous vigorous stirring. After vigorously stirring this suspension for 15 min, 4-hydroxy-benzaldehyde (1.7 g, 8 equiv.) dissolved in dry THF (10 mL) was added. The resultant reaction mixture was heated to reflux for 48 h. The reaction mixture was concentrated in vacuum, and the residue obtained was purified by column chromatography using silica gel with an eluent made of mixing hexane and ethyl acetate (v/v 100/50). Yield = 60 %. HRMS (ESI) m/z: $(M + H)^+$ calculated for $C_{42}H_{31}N_3O_{12}P_3$ 862.1120. Found 862.1093.

NMR of Compound 1

^{1}H NMR (400 MHz, $CDCl_3$, δ in ppm) 9.93 (s, 6H), 7.73 (d, J = 8.5 Hz, 12H), 7.14 (d, J = 8.5 Hz, 12H).

^{13}C NMR (100 MHz, $CDCl_3$, δ in ppm) 190.44, 154.48, 133.77, 131.42, 121.25, 121.23.

FTIR (cm^{-1})

1703.9, 1598.1, 1500.4, 1421.6, 1390.3, 1299.9, 1274.1, 1207.2, 1177.4, 1155.2, 1101.4, 1012.2, 952.7, 887.8, 839.5, 761.5, 707.7, 609.2, 557.2, 514.5

NMR Spectrum

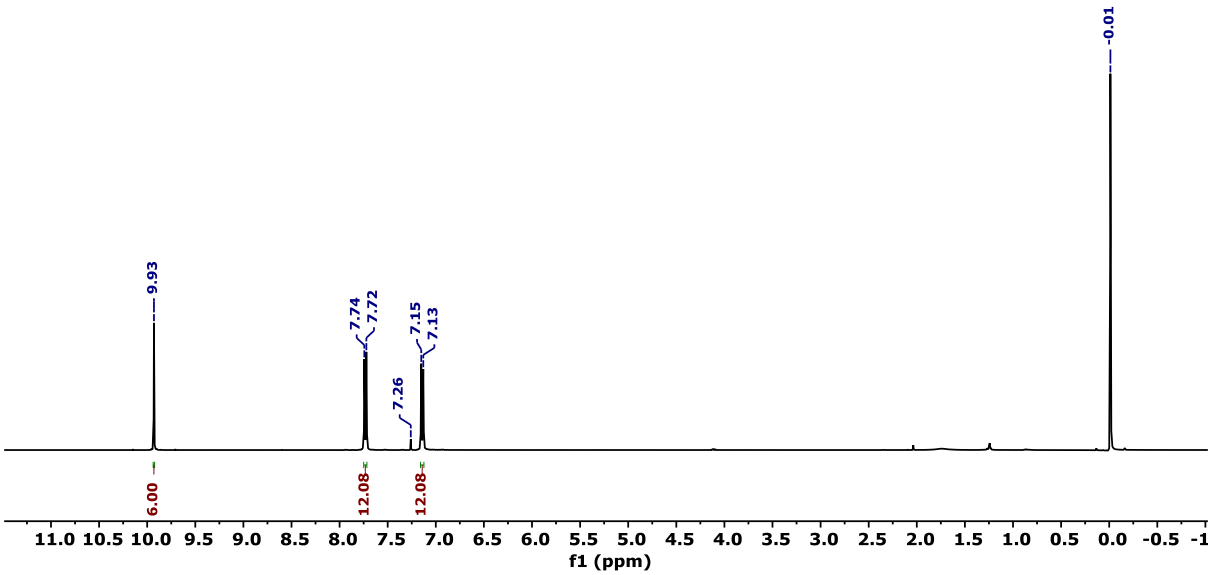

Fig. S1 ^{1}H NMR spectrum of compound **1** in $CDCl_3$.

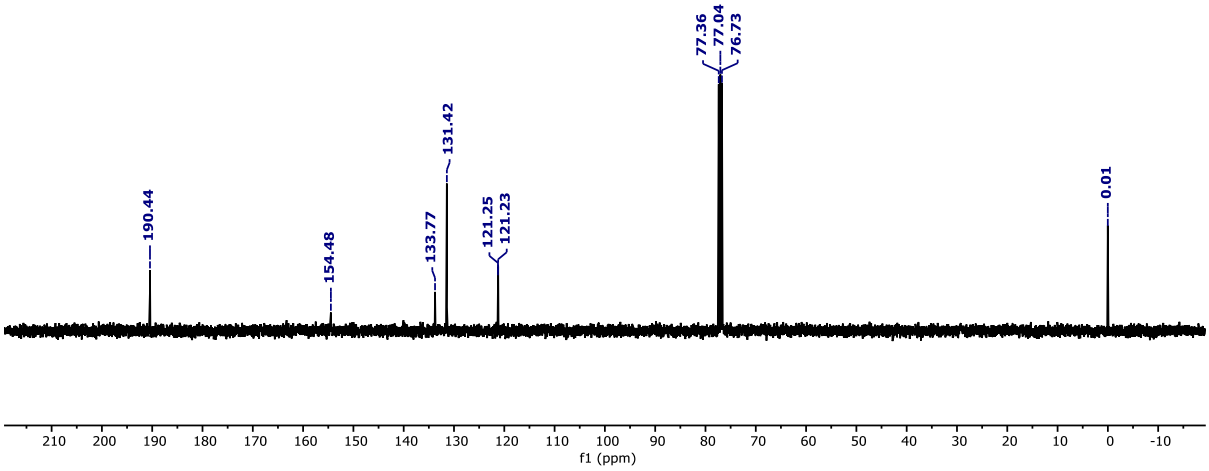

Fig. S2 ^{13}C NMR spectrum of compound **1** in $CDCl_3$.

Mass Spectrum

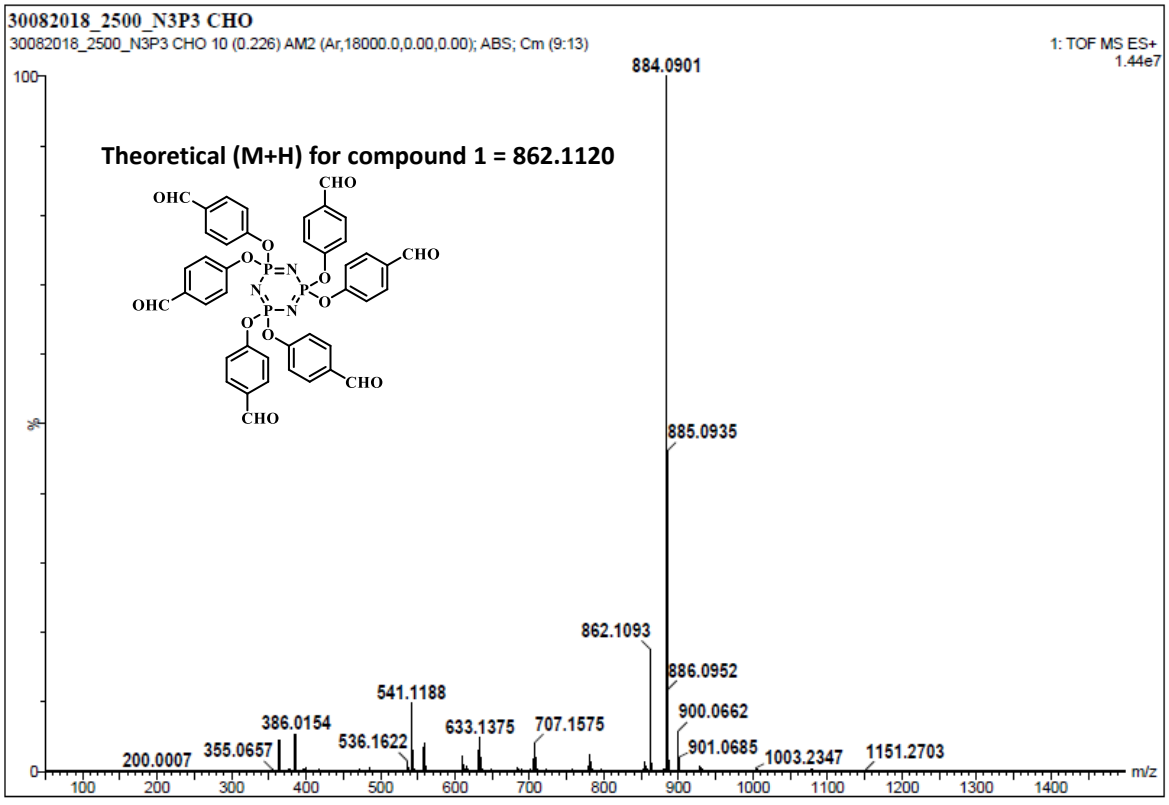

Fig. S3 HRMS spectrum of compound **1**.

Synthesis of compound 2(a - f):

Cholesterol (1.2 equiv.) was added to the stirred solution of bromoalkanoic acid (2 g, 1 equiv.) in dry DCM (40 mL). The resulting mixture was stirred under a nitrogen atmosphere, and DMAP (catalytic amount) was added to the solution. A solution of DCC (1.25 equiv.) in DCM was further added to the reaction mixture, and the mixture was stirred at 60 °C for 12 h. The reaction mixture was filtered, and the filtrate obtained was concentrated in a vacuum. The

crude product was then purified by column chromatography using silica gel with a mixture of hexane/ethyl acetate (v/v, 100/1) as an eluent. The white solid obtained was air-dried and stored in a clean sample vial. Yield = 75 – 78 %.

Characterization details of 2(a - f)

2a: Yield = 76 %, ^{1}H NMR (400 MHz, $CDCl_3$, δ in ppm) 5.37 (d, J = 5.5 Hz, 1H), 4.65 – 4.59 (m, 1H), 3.41 (t, J = 6.8 Hz, 2H), 2.35 – 2.25 (m, 4H), 1.99 (s, 2H), 1.92 – 1.79 (m, 5H), 1.69 – 1.62 (m, 2H), 1.59 – 1.44 (m, 8H), 1.39 – 1.25 (m, 4H), 1.20 – 1.04 (m, 8H), 1.02 (s, 4H), 0.97 (d, J = 11.0 Hz, 2H), 0.91 (d, J = 6.5 Hz, 3H), 0.86 (dd, J = 6.6, 1.9 Hz, 6H), 0.68 (s, 3H).

^{13}C NMR (100 MHz, $CDCl_3$, δ in ppm) 172.89, 139.66, 122.67, 73.89, 56.69, 56.14, 50.03, 42.32, 39.73, 39.53, 38.16, 37.00, 36.60, 36.19, 35.80, 34.43, 33.52, 32.42, 31.91, 31.87, 28.24, 28.03, 27.82, 27.63, 24.29, 24.18, 23.84, 22.84, 22.58, 21.04, 19.33, 18.73, 11.87.

FTIR (cm^{-1}) 2949, 2888, 2867, 2850, 1733, 1467, 1434, 1373, 1324, 1255, 1190, 1174.

2b: Yield = 75 %, ^{1}H NMR (400 MHz, $CDCl_3$, δ in ppm) 5.37 (d, J = 5.0 Hz, 1H), 4.62 – 4.58 (m, 1H), 3.44 – 3.38 (m, 2H), 2.29 (q, J = 7.5 Hz, 4H), 2.04 – 1.93 (m, 2H), 1.90 – 1.80 (m, 5H), 1.67 – 1.52 (m, 7H), 1.46 (ddd, J = 14.2, 7.5, 4.5 Hz, 6H), 1.35 (h, J = 6.2, 5.3 Hz, 5H), 1.25 (d, J = 4.4 Hz, 1H), 1.13 (ddd, J = 19.4, 13.0, 7.4 Hz, 6H), 1.02 (s, 4H), 0.98 (d, J = 4.9 Hz, 1H), 0.91 (d, J = 6.5 Hz, 3H), 0.86 (dd, J = 6.6, 1.9 Hz, 6H), 0.68 (s, 3H).

^{13}C NMR (100 MHz, $CDCl_3$, δ in ppm) 173.09, 139.67, 122.66, 73.81, 56.69, 56.13, 50.02, 42.32, 39.73, 39.53, 38.17, 37.00, 36.61, 36.19, 35.81, 34.53, 33.82, 32.56, 31.92, 31.86, 28.25, 28.22, 28.03, 27.82, 24.82, 24.30, 23.84, 22.85, 22.59, 21.04, 19.35, 18.73, 11.87.

FTIR (cm^{-1}) 2946, 2888, 2868, 2848, 1732, 1465, 1435, 1376, 1324, 1247, 1187, 1172.

2c: Yield = 78 %, ^{1}H NMR (400 MHz, $CDCl_3$, δ in ppm) 5.37 (d, J = 5.4 Hz, 1H), 4.67 – 4.57 (m, 1H), 3.40 (t, J = 6.8 Hz, 2H), 2.34 – 2.24 (m, 4H), 2.04 – 1.93 (m, 2H), 1.89 – 1.78 (m, 5H), 1.65 – 1.53 (m, 7H), 1.52 – 1.39 (m, 6H), 1.33 (p, J = 3.7 Hz, 7H), 1.28 – 1.21 (m, 1H), 1.13 (ddd, J = 19.3, 9.7, 5.8 Hz, 6H), 1.02 (s, 4H), 0.96 (t, J = 5.8 Hz, 1H), 0.91 (d, J = 6.5 Hz, 3H), 0.86 (dd, J = 6.6, 1.9 Hz, 6H), 0.68 (s, 3H).

^{13}C NMR (100 MHz, $CDCl_3$, δ in ppm) 173.18, 139.69, 122.63, 73.76, 56.69, 56.14, 50.03, 42.32, 39.74, 39.53, 38.17, 37.01, 36.60, 36.19, 35.81, 34.61, 33.89, 32.72, 31.91, 31.87, 28.90, 28.42, 28.25, 28.03, 27.99, 27.83, 24.91, 24.30, 23.84, 22.84, 22.58, 21.04, 19.34, 18.73, 11.87.

FTIR (cm^{-1}) 2945, 2888, 2869, 1733, 1559, 1543, 1468, 1440, 1367, 1242, 1184, 1173.

2d: Yield = 75 %, ^{1}H NMR (400 MHz, $CDCl_3$, δ in ppm) 5.37 (d, J = 5.0 Hz, 1H), 4.66 – 4.57 (m, 1H), 3.40 (t, J = 6.8 Hz, 2H), 2.33 – 2.24 (m, 4H), 2.04 – 1.92 (m, 2H), 1.89 – 1.78 (m, 5H), 1.65 – 1.52 (m, 6H), 1.52 – 1.48 (m, 2H), 1.45 – 1.39 (m, 3H), 1.32 (d, J = 5.0 Hz, 10H), 1.13 (ddd, J = 19.6, 13.5, 5.7 Hz, 7H), 1.02 (s, 5H), 0.97 (d, J = 11.0 Hz, 1H), 0.91 (d, J = 6.4 Hz, 3H), 0.86 (dd, J = 6.6, 1.9 Hz, 6H), 0.68 (s, 3H).

^{13}C NMR (100 MHz, $CDCl_3$, δ in ppm) 173.25, 139.70, 122.62, 73.73, 56.69, 56.13, 50.02, 42.31, 39.73, 39.53, 38.17, 37.01, 36.60, 36.19, 35.81, 34.67, 34.00, 32.79, 31.92, 31.86, 29.08,

28.99, 28.59, 28.25, 28.11, 28.03, 27.83, 24.99, 24.30, 23.84, 22.85, 22.59, 21.04, 19.35, 18.73, 11.87.

FTIR (cm^{-1}) 2942, 2889, 2866, 2852, 1736, 1466, 1435, 1375, 1263, 1228, 1172.

2e: Yield = 77 %, ^{1}H NMR (400 MHz, $CDCl_3$, δ in ppm) 5.37 (d, *J* = 5.0 Hz, 1H), 4.67 – 4.54 (m, 1H), 3.40 (t, *J* = 6.9 Hz, 2H), 2.34 - 2.22 (m, 4H), 2.03 - 1.93 (m, 2H), 1.90 - 1.79 (m, 5H), 1.66 - 1.47 (m, 8H), 1.46 - 1.39 (m, 5H), 1.28 (s, 12H), 1.16 - 1.10 (m, 7H), 1.01 (s, 6H), 0.91 (d, *J* = 6.5 Hz, 3H), 0.86 (dd, *J* = 6.7, 1.9 Hz, 6H), 0.67 (s, 3H).

^{13}C NMR (100 MHz, $CDCl_3$, δ in ppm) 173.33, 139.72, 122.62, 73.70, 56.69, 56.13, 50.02, 42.32, 39.73, 39.53, 38.17, 37.01, 36.61, 36.19, 35.81, 34.72, 34.08, 32.84, 31.92, 31.86, 29.37, 29.34, 29.22, 29.09, 28.75, 28.25, 28.18, 28.03, 27.83, 25.05, 24.30, 23.84, 22.85, 22.59, 21.04, 19.35, 18.73, 11.87.

FTIR (cm^{-1}) 2941, 2889, 2868, 2852, 1736, 1599, 1577, 1467, 1438, 1380, 1364, 1168.

2f: Yield = 76 %, ^{1}H NMR (400 MHz, $CDCl_3$, δ in ppm) 5.37 (d, *J* = 5.0 Hz, 1H), 4.63 – 4.57 (m, 1H), 3.40 (td, *J* = 6.9, 1.9 Hz, 2H), 2.33 – 2.23 (m, 4H), 1.98 (t, *J* = 15.5 Hz, 2H), 1.84 (p, *J* = 6.3, 5.7 Hz, 5H), 1.60 – 1.52 (m, 4H), 1.49 (q, *J* = 8.9, 7.5 Hz, 3H), 1.41 (t, *J* = 7.5 Hz, 3H), 1.30 (d, *J* = 18.9 Hz, 18H), 1.12 (ddd, *J* = 20.1, 13.1, 6.9 Hz, 6H), 1.01 (s, 5H), 0.96 (d, *J* = 11.1 Hz, 1H), 0.91 (d, *J* = 6.4 Hz, 3H), 0.86 (d, *J* = 6.6 Hz, 6H), 0.67 (s, 3H).

^{13}C NMR (100 MHz, $CDCl_3$, δ in ppm) 173.34, 139.72, 122.61, 73.70, 56.69, 56.13, 50.03, 42.32, 39.74, 39.53, 38.17, 37.01, 36.61, 36.19, 35.81, 34.72, 34.06, 32.85, 31.92, 31.87, 29.46, 29.41, 29.25, 29.11, 28.77, 28.25, 28.19, 28.03, 27.83, 25.06, 24.30, 23.84, 22.84, 22.58, 21.04, 19.34, 18.73, 11.87.

FTIR (cm^{-1}) 2944, 2886, 2869, 2851, 1737, 1649, 1554, 1467, 1461, 1381, 1365, 1172.

Synthesis of compound 3(a - f)

Potassium carbonate (5 equiv.) was added to the solution of 4-nitrophenol (1.5 equiv.) in n-butanone. The above suspension was stirred for 15 min, and then compound **2** (3.5 g, 1 equiv.) was added, followed by the addition of potassium iodide (KI) in a catalytic amount. The reaction mixture was refluxed and continuously stirred for 24 h. The crude product was poured into ice-cold water and extracted with DCM. The organic phase dried over Na_2SO_4 was concentrated in vacuum. The crude product obtained was purified by column chromatography using silica gel with a mixture of hexane/ethyl acetate (v/v 100/2.5) as eluent. Yield = 85 – 90 %.

Characterization details of 3(a - f)

3a: Yield = 87 %, ^{1}H NMR (400 MHz, $CDCl_3$, δ in ppm) 8.19 (d, *J* = 9.2 Hz, 2H), 6.93 (d, *J* = 9.3 Hz, 2H), 5.37 (d, *J* = 5.8 Hz, 1H), 4.67 - 4.57 (m, 1H), 4.05 (t, *J* = 6.4 Hz, 2H), 2.36 - 2.25 (m, 4H), 2.04 - 1.93 (m, 2H), 1.89 - 1.79 (m, 5H), 1.70 (q, *J* = 7.6 Hz, 2H), 1.60 (s, 3H), 1.57 - 1.40 (m, 8H), 1.37 - 1.27 (m, 3H), 1.16 - 1.07 (m, 7H), 1.01 (s, 5H), 0.91 (d, *J* = 6.5 Hz, 3H), 0.86 (dd, *J* = 6.6, 1.9 Hz, 6H), 0.67 (s, 3H).

^{13}C NMR (100 MHz, $CDCl_3$, δ in ppm) 172.94, 164.12, 141.37, 139.61, 125.93, 122.71, 114.39, 73.90, 68.52, 56.69, 56.13, 50.02, 42.32, 39.73, 39.52, 38.17, 36.98, 36.60, 36.19, 35.80, 34.48, 31.91, 31.86, 28.68, 28.24, 28.02, 27.82, 25.48, 24.68, 24.29, 23.84, 22.84, 22.58, 21.04, 19.32, 18.73, 11.87.

FTIR (cm^{-1}) 2962, 2946, 2904, 2888, 2868, 1731, 1594, 1517, 1468, 1342, 1267, 1174, 1110, 1031, 845, 750.

3b: Yield = 85 %, ^{1}H NMR (400 MHz, $CDCl_3$, δ in ppm) 8.19 (d, *J* = 9.2 Hz, 2H), 6.93 (d, *J* = 9.2 Hz, 2H), 5.35 (d, *J* = 5.1 Hz, 1H), 4.66 – 4.57 (m, 1H), 4.04 (t, *J* = 6.4 Hz, 2H), 2.32 – 2.26 (m, 4H), 2.03 – 1.93 (m, 2H), 1.83 (m, 6H), 1.65 (q, *J* = 7.4 Hz, 3H), 1.49 (q, *J* = 7.6, 7.1 Hz, 6H), 1.43 – 1.37 (m, 3H), 1.36 – 1.31 (m, 3H), 1.25 (d, *J* = 3.7 Hz, 1H), 1.12 (ddd, *J* = 19.0, 13.4, 6.8 Hz, 8H), 1.01 (s, 4H), 0.96 (d, *J* = 11.7 Hz, 1H), 0.91 (d, *J* = 6.5 Hz, 3H), 0.86 (dd, *J* = 6.6, 1.9 Hz, 6H), 0.67 (s, 3H).

^{13}C NMR (100 MHz, $CDCl_3$, δ in ppm) 173.11, 164.18, 141.34, 139.62, 125.94, 122.69, 114.39, 73.82, 68.6, 56.68, 56.12, 50.01, 42.31, 39.72, 39.52, 38.17, 36.98, 36.60, 36.18, 35.80, 34.53, 31.90, 31.85, 28.78, 28.73, 28.24, 28.03, 27.82, 25.62, 24.88, 24.29, 23.83, 22.84, 22.58, 21.03, 19.33, 18.72, 11.86.

FTIR (cm^{-1}) 2954, 2941, 2898, 2887, 2869, 1734, 1593, 1510, 1471, 1342, 1271, 1176, 1110, 1027, 1005, 848, 748.

3c: Yield = 89 %, ^{1}H NMR (400 MHz, $CDCl_3$, δ in ppm) 8.19 (d, *J* = 8.7 Hz, 2H), 6.93 (d, *J* = 8.7 Hz, 2H), 5.36 (d, *J* = 5.0 Hz, 1H), 4.60 (m, 1H), 4.03 (t, *J* = 6.5 Hz, 2H), 2.32 – 2.25 (m, 4H), 1.98 (t, *J* = 16.1 Hz, 2H), 1.88 – 1.77 (m, 5H), 1.65 – 1.53 (m, 6H), 1.51 – 1.42 (m, 6H), 1.39 – 1.32 (m, 6H), 1.25 (d, *J* = 6.8 Hz, 2H), 1.12 (ddd, *J* = 19.7, 13.3, 6.7 Hz, 7H), 1.01 (s, 4H), 0.96 (d, *J* = 11.4 Hz, 1H), 0.91 (d, *J* = 6.4 Hz, 3H), 0.86 (d, *J* = 6.7 Hz, 6H), 0.67 (s, 3H).

^{13}C NMR (100 MHz, $CDCl_3$, δ in ppm) 173.20, 164.21, 141.32, 139.66, 125.93, 122.66, 114.39, 73.78, 68.79, 56.68, 56.13, 50.02, 42.31, 39.73, 39.52, 38.18, 37.00, 36.60, 36.19, 35.80, 34.61, 31.91, 31.86, 28.96, 28.94, 28.90, 28.24, 28.03, 27.83, 25.74, 24.91, 24.29, 23.84, 22.84, 22.58, 21.04, 19.33, 18.73, 11.87.

FTIR (cm^{-1}) 2941, 2931, 2887, 2870, 2847, 1736, 1592, 1516, 1467, 1343, 1265, 1172, 1112, 1031, 1007, 845, 753.

3d: Yield = 90 %, ^{1}H NMR (400 MHz, $CDCl_3$, δ in ppm) 8.20 (d, *J* = 9.2 Hz, 2H), 6.94 (d, *J* = 9.2 Hz, 2H), 5.36 (d, *J* = 5 Hz, 1H), 4.64 – 4.60 (m, 1H), 4.04 (t, *J* = 6.5 Hz, 2H), 2.33 – 2.26 (m, 4H), 2.03 – 1.94 (m, 2H), 1.87 – 1.79 (m, 5H), 1.61 (d, *J* = 7.4 Hz, 2H), 1.54 – 1.42 (m, 8H), 1.39 – 1.30 (m, 10H), 1.25 (d, *J* = 4.3 Hz, 1H), 1.13 (td, *J* = 11.2, 10.1, 5.1 Hz, 7H), 1.01 (s, 5H), 0.99 – 0.96 (m, 1H), 0.91 (d, *J* = 6.5 Hz, 3H), 0.86 (dd, *J* = 6.6, 1.9 Hz, 6H), 0.67 (s, 3H).

^{13}C NMR (100 MHz, $CDCl_3$, δ in ppm) 173.2, 164.24, 141.31, 139.68, 125.94, 122.66, 114.40, 73.75, 68.84, 56.68, 56.12, 50.01, 42.31, 39.72, 39.53, 38.18, 37.00, 36.61, 36.19, 35.81, 34.66, 31.91, 31.86, 29.14, 29.10, 28.98, 28.95, 28.25, 28.03, 27.83, 25.85, 24.99, 24.29, 23.84, 22.85, 22.58, 21.04, 19.34, 18.73, 11.87.

FTIR (cm^{-1}) 2963, 2948, 2900, 2885, 2869, 1735, 1593, 1507, 1471, 1339, 1268, 1176, 1112, 1019, 849, 751.

3e: Yield = 85 %, ^{1}H NMR (400 MHz, $CDCl_3$, δ in ppm) 8.20 (d, J = 9.2 Hz, 2H), 6.94 (d, J = 9.3 Hz, 2H), 5.37 (d, J = 5.0 Hz, 1H), 4.65 - 4.57 (m, 1H), 4.04 (t, J = 6.5 Hz, 2H), 2.32 - 2.25 (m, 4H), 2.03 - 1.93 (m, 2H), 1.87 - 1.78 (m, 5H), 1.60 (s, 4H), 1.53 - 1.43 (m, 6H), 1.36 - 1.25 (m, 15H), 1.20 - 1.06 (m, 8H), 1.02 (s, 4H), 0.99 - 0.96 (m, 1H), 0.91 (d, J = 6.5 Hz, 3H), 0.86 (dd, J = 6.6, 1.9 Hz, 6H), 0.67 (s, 3H).

^{13}C NMR (100 MHz, $CDCl_3$, δ in ppm) 173.31, 164.25, 141.30, 139.70, 125.92, 122.62, 114.39, 73.71, 68.88, 56.68, 56.12, 50.01, 42.31, 39.72, 39.52, 38.17, 37.00, 36.60, 36.18, 35.80, 34.70, 31.91, 31.86, 29.44, 29.33, 29.27, 29.22, 29.08, 28.97, 28.24, 28.03, 27.82, 25.91, 25.03, 24.29, 23.83, 22.84, 22.58, 21.03, 19.34, 18.72, 11.86.

FTIR (cm^{-1}) 2946, 2939, 2886, 2869, 2852, 1734, 1594, 1517, 1470, 1340, 1266, 1172, 1112, 1010, 848, 753.

3f: Yield = 87 %, ^{1}H NMR (400 MHz, $CDCl_3$, δ in ppm) 8.19 (d, J = 7.3 Hz, 2H), 6.93 (d, J = 8.7 Hz, 2H), 5.36 (d, J = 5.0 Hz, 1H), 4.62 – 4.59 (m, 1H), 4.04 (t, J = 6.6 Hz, 2H), 2.31 - 2.24 (m, 4H), 2.05 - 1.93 (m, 3H), 1.82 (q, J = 9.9, 7.4 Hz, 6H), 1.57 (dd, J = 20.1, 9.6 Hz, 6H), 1.46 (q, J = 9.1, 7.9 Hz, 6H), 1.28 (s, 12H), 1.16 - 1.09 (m, 8H), 1.01 (s, 4H), 0.97 (s, 1H), 0.94 (d, J = 5.7 Hz, 1H), 0.91 (d, J = 6.4 Hz, 3H), 0.87 (s, 6H), 0.67 (s, 3H).

^{13}C NMR (100 MHz, $CDCl_3$, δ in ppm) 173.33, 16.26, 141.31, 139.71, 125.93, 122.62, 114.40, 73.71, 68.89, 56.69, 56.13, 50.02, 42.31, 39.73, 39.53, 38.18, 37.01, 36.61, 36.19, 35.81, 34.71, 31.91, 31.86, 29.72, 29.49, 29.41, 29.31, 29.25, 29.10, 28.98, 28.24, 28.03, 27.83, 25.92, 25.05, 24.29, 23.84, 22.72, 22.84, 22.58, 21.04, 19.34, 18.72, 11.86.

FTIR (cm^{-1}) 2936, 2886, 2870, 2853, 1736, 1595, 1519, 1469, 1341, 1262, 1173, 1113, 1020, 848, 751.

Synthesis of compound 4(a - f)

The procedure for the synthesis of compound 4(a - f) is similar, as reported in the literature.[5] Compound 3 (2 g, 1equiv.) was dissolved in a minimum amount of dry THF. To the above solution, 10 % Pd/C was added, and the mixture was stirred under H_2 atmosphere. The reaction was monitored with the help of TLC; the reaction was found to be completed after 48 h of stirring. After completion of the reaction, the mixture was filtered through a celite/silica gel bed and the product obtained after the evaporation of the solvent under vacuum was directly used for the next step without any purification.

Synthesis of compounds P-n

The final Schiff base compounds were synthesized by refluxing a mixture of compounds **4** (467 mg, 7 equiv.) and **1** (100 mg, 1 equiv.) in dry THF for 24 h. The crude product was obtained by evaporating the solvent in vacuum. The residue obtained was purified by recrystallization technique using a mixture of DCM and methanol (1:9). Yield = 35 - 40 %.

Characterization details of final compounds

P-5: Yield = 39 %, UV-vis (absorbance in nm): 273, 338, Fluorescence: 377, 407, 431. ^{1}H NMR (400 MHz, $CDCl_3$, δ in ppm) 8.37 (s, 6H), 7.72 (d, *J* = 8.6 Hz, 12H), 7.10 (dd, *J* = 26.4, 8.6 Hz, 24H), 6.82 (d, *J* = 8.9 Hz, 12H), 5.37 (d, *J* = 5.0 Hz, 6H), 4.66 – 4.58 (m, 6H), 3.96 (t, *J* = 6.4 Hz, 12H), 2.33 (dd, *J* = 9.0, 6.3 Hz, 24H), 2.02 – 1.93 (m, 12H), 1.83 (q, *J* = 8.9, 8.1 Hz, 36H), 1.72 (p, *J* = 7.6 Hz, 18H), 1.57 – 1.45 (m, 54H), 1.34 (d, *J* = 8.0 Hz, 18H), 1.25 (d, *J* = 6.7 Hz, 6H), 1.12 (dt, *J* = 14.2, 10.6 Hz, 42H), 1.01 (s, 24H), 0.91 (d, *J* = 6.5 Hz, 18H), 0.86 (dd, *J* = 6.6, 1.9 Hz, 36H), 0.67 (s, 18H).

^{13}C NMR (100 MHz, $CDCl_3$, δ in ppm) 173.04, 157.82, 156.57, 152.22, 144.34, 139.67, 133.70, 129.93, 122.66, 122.29, 121.24, 121.21, 114.92, 73.84, 67.87, 56.69, 56.13, 50.02, 42.31, 39.73, 39.53, 38.18, 37.01, 36.60, 36.20, 35.82, 34.59, 31.92, 31.86, 29.06, 28.26, 28.03, 27.84, 25.68, 24.85, 24.30, 23.85, 22.86, 22.60, 21.05, 19.35, 18.74, 11.88.

FTIR (cm^{-1}) 2936.1, 2866.6, 2851.4, 1732.8, 1626.5, 1602.5, 1574.1, 1506.6, 1467.5, 1378.15, 1258.5, 1208.5, 1173.6, 1106.1, 1014.6, 958.3, 883.7, 844.1, 746.9, 603.9, 569.7, 542.1.

P-6: Yield = 35 %, UV-vis (absorbance in nm): 273, 338, Fluorescence: 377, 407, 431. ^{1}H NMR (400 MHz, $CDCl_3$, δ in ppm) 8.37 (s, 6H), 7.71 (d, *J* = 8.5 Hz, 12H), 7.10 (dd, *J* = 27.3, 8.6 Hz, 24H), 6.83 (d, *J* = 8.9 Hz, 12H), 5.37 (d, *J* = 8.0 Hz, 6H), 4.64 - 4.59 (m, 6H), 3.95 (t, *J* = 6.5 Hz, 12H), 2.31 (d, *J* = 7.8 Hz, 24H), 2.01 - 1.94 (m, 12H), 1.86 - 1.78 (m, 36H), 1.67 (t, *J* = 7.6 Hz, 12H), 1.57 - 1.47 (m, 48H), 1.44 - 1.41 (m, 12H), 1.36 - 1.32 (m, 18H), 1.26 - 1.23 (m, 6H), 1.16 - 1.07 (m, 48H), 1.01 (s, 24H), 0.98 (s, 6H), 0.91 (d, *J* = 6.6 Hz, 18H), 0.86 (dd, *J* = 6.6, 1.9 Hz, 36H), 0.67 (s, 18H).

^{13}C NMR (100 MHz, $CDCl_3$, δ in ppm) 173.17, 157.88, 156.53, 152.28, 144.31, 139.84, 139.68, 131.45, 129.93, 122.65, 122.30, 121.22, 116.43, 115.64, 114.93, 73.78, 68.04, 56.69, 56.13, 50.02, 42.31, 39.73, 39.53, 38.18, 37.00, 36.60, 36.19, 35.82, 34.63, 31.92, 31.86, 29.20, 28.25, 28.04, 27.84, 25.82, 24.99, 24.30, 23.85, 22.86, 22.59, 21.04, 19.35, 18.73, 11.88.

FTIR (cm^{-1}) 2935.7, 2867.8, 2853.7, 1732.7, 1624.9, 1603.9, 1576.6, 1507.4, 1465.6, 1376.9, 1249.6, 1210.7, 1173.8, 1108.6, 1013.5, 965.7, 883.1, 794.8, 734.9, 607.9, 570.9, 546.3.

P-7: Yield = 37 %, UV-vis (absorbance in nm): 273, 338, Fluorescence: 377, 407, 431. ^{1}H NMR (400 MHz, $CDCl_3$, δ in ppm) 8.37 (s, 6H), 7.71 (d, *J* = 8.5 Hz, 12H), 7.10 (dd, *J* = 26.3, 8.6 Hz, 24H), 6.83 (d, *J* = 8.9 Hz, 12H), 5.37 (d, *J* = 8.0 Hz, 6H), 4.65 – 4.59 (m, 6H), 3.95 (t, J = 6.6 Hz, 12H), 2.32 – 2.27 (m, 24H), 2.02 – 1.93 (m, 12H), 1.83 (ddd, *J* = 24.2, 12.6, 5.1 Hz, 36H), 1.64 (t, *J* = 7.2 Hz, 18H), 1.52 – 1.44 (m, 36H), 1.43 (d, *J* = 4.8 Hz, 6H), 1.40 – 1.31 (m, 48H), 1.25 (d, *J* = 9.8 Hz, 6H), 1.17 – 1.04 (m, 48H), 1.01 (s, 24H), 0.91 (d, *J* = 6.6 Hz, 18H), 0.86 (dd, *J* = 6.6, 1.9 Hz, 36H), 0.67 (s, 18H).

^{13}C NMR (100 MHz, $CDCl_3$, δ in ppm) 173.20, 157.91, 139.71, 129.91, 122.62, 122.27, 121.22, 114.95, 73.74, 68.15, 56.70, 56.15, 50.04, 42.32, 39.74, 39.53, 38.19, 37.02, 36.61, 36.20, 35.81, 34.67, 31.87, 29.32, 29.08, 28.24, 28.02, 27.84, 25.95, 25.00, 24.29, 23.85, 22.83, 22.58, 21.05, 19.34, 18.73, 11.87.

FTIR (cm^{-1}) 2934.8, 2866.4, 2852.2, 1732.5, 1625.1, 1604.6, 1577.8, 1507.6, 1467.9, 1377.2, 1249.9, 1207.5, 1173.8, 1107, 1012.7, 960.5, 881.5, 841.8, 796.9, 764.1, 749.7, 607, 545.5.

P-8: Yield = 40 %, UV-vis (absorbance in nm): 273, 338, Fluorescence: 377, 407, 431. ^{1}H NMR (400 MHz, $CDCl_3$, δ in ppm) 8.37 (s, 6H), 7.71 (d, *J* = 8.4 Hz, 12H), 7.10 (dd, *J* = 26.9, 8.6 Hz, 24H), 6.83 (d, *J* = 8.9 Hz, 12H), 5.37 (d, *J* = 8.0 Hz, 6H), 4.63 – 4.59 (m, 6H), 3.95 (t, *J* = 6.5 Hz, 12H), 2.29 (q, *J* = 6.8, 5.3 Hz, 24H), 2.02 – 1.95 (m, 12H), 1.84 (ddd, *J* = 18.5, 11.0, 5.3 Hz, 36H), 1.65 – 1.59 (m, 18H), 1.56 (d, *J* = 3.2 Hz, 6H), 1.53 (d, *J* = 3.0 Hz, 6H), 1.52 – 1.45 (m, 36H), 1.43 (d, *J* = 4.5 Hz, 6H), 1.37 – 1.32 (m, 54H), 1.27 – 1.23 (m, 6H), 1.16 – 1.07 (m, 42H), 1.02 (s, 24H), 0.91 (d, *J* = 6.4 Hz, 18H), 0.87 – 0.85 (m, 36H), 0.67 (d, *J* = 1.9 Hz, 18H).

^{13}C NMR (100 MHz, $CDCl_3$, δ in ppm) 173.28, 157.93, 156.50, 144.26, 139.70, 133.72, 131.45, 129.93, 122.63, 122.29, 121.23, 116.44, 115.64, 115.00, 114.93, 73.73, 68.63, 68.19, 56.69, 56.26, 56.13, 50.02, 42.32, 39.73, 39.53, 38.18, 37.01, 36.61, 36.19, 35.82, 34.71, 31.92, 31.86, 29.37, 29.31, 29.26, 29.22, 29.10, 28.26, 28.04, 27.84, 26.07, 25.06, 24.31, 23.85, 22.86, 22.60, 21.05, 19.35, 18.74, 11.88.

FTIR (cm^{-1}) 2933, 2867.6, 2852.5, 1733.8, 1624.6, 1603.9, 1578.1, 1507, 1467.2, 1377.3, 1275.3, 1259.7, 1211.3, 1175, 1109.2, 1101.2, 964.4, 881.5, 841.2, 794.5, 750.3, 609.4, 546.9.

P-10: Yield = 36 %, UV-vis (absorbance in nm): 273, 338, Fluorescence: 377, 407, 431. ^{1}H NMR (400 MHz, $CDCl_3$, δ in ppm) 8.37 (s, 6H), 7.71 (d, *J* = 8.6 Hz, 12H), 7.09 (dd, *J* = 25.9, 8.6 Hz, 24H), 6.83 (d, *J* = 8.9 Hz, 12H), 5.37 (d, *J* = 5.0 Hz, 6H), 4.64 - 4.58 (m, 6H), 3.95 (t, *J* = 6.6 Hz, 12H), 2.32 - 2.25 (m, 24H), 2.02 - 1.94 (m, 12H), 1.88 - 1.75 (m, 36H), 1.62 - 1.60 (m, 12H), 1.57 - 1.53 (m, 12H), 1.50 - 1.42 (m, 42H), 1.31 (d, *J* = 2.9 Hz, 78H), 1.25 (d, *J* = 7.6 Hz, 6H), 1.16 - 1.07 (m, 36H), 1.02 (s, 24H), 0.96 (dd, *J* = 13.5, 3.6 Hz, 12H), 0.91 (d, *J* = 6.5 Hz, 18H), 0.86 (dd, *J* = 6.6, 1.9 Hz, 36H), 0.67 (s, 18H).

^{13}C NMR (100 MHz, $CDCl_3$, δ in ppm) 173.33, 157.94, 156.51, 152.22, 144.26, 139.72, 133.72, 129.92, 122.62, 122.29, 121.23, 116.43, 115.00, 114.93, 73.70, 68.24, 56.69, 56.13, 50.01, 42.31, 39.73, 39.53, 38.18, 37.01, 36.61, 36.19, 35.82, 34.73, 31.92, 31.86, 29.57, 29.46, 29.41, 29.31, 29.16, 28.25, 28.04, 27.83, 26.13, 25.08, 24.30, 23.85, 22.86, 22.59, 21.04, 19.35, 18.73, 11.88.

FTIR (cm^{-1}) 2932.2, 2869.4, 2852.4, 1733.3, 1625.6, 1604.4, 1577.1, 1507.3, 1467.1, 1376.37, 1275, 1260.3, 1207.5, 1173.6, 1108.1, 1015.7, 964.5, 880.6, 842, 765.1, 749.4, 605.4, 547.1.

P-11: Yield = 36 %, UV-vis (absorbance in nm): 273, 338, Fluorescence: 377, 407, 431. ^{1}H NMR (400 MHz, $CDCl_3$, δ in ppm) 8.37 (s, 6H), 7.71 (d, *J* = 8.7 Hz, 12H), 7.09 (dd, *J* = 25.5, 8.6 Hz, 24H), 6.82 (d, *J* = 8.9 Hz, 12H), 5.37 (d, *J* = 5.0 Hz, 6H), 4.62 - 4.58 (m, 6H), 3.94 (t, *J* = 6.7 Hz, 12H), 2.32 - 2.25 (m, 24H), 2.02 - 1.94 (m, 12H), 1.86 - 1.76 (m, 36H), 1.61 (s, 12H), 1.56 (t, *J* = 2.4 Hz, 6H), 1.51 - 1.42 (m, 42H), 1.30 (d, *J* = 3.8 Hz, 90H), 1.17 - 1.06 (m, 48H), 1.01 (s, 24H), 0.98 - 0.96 (m, 6H), 0.94 (d, *J* = 5.5 Hz, 6H), 0.91 (d, *J* = 6.6 Hz, 18H), 0.86 (dd, *J* = 6.6, 1.9 Hz, 36H), 0.67 (s, 18H).

^{13}C NMR (100 MHz, $CDCl_3$, δ in ppm) 173.35, 157.95, 139.72, 129.93, 122.61, 122.29, 121.21, 116.43, 115.65, 115.00, 114.93, 73.70, 68.24, 56.69, 56.13, 50.02, 42.31, 39.73, 39.53,

38.18, 37.01, 36.61, 36.19, 35.82, 34.74, 31.92, 31.86, 29.61, 29.51, 29.32, 29.16, 28.25, 28.04, 27.83, 25.09, 24.30, 23.85, 22.85, 22.59, 21.04, 19.35, 18.73, 11.87.

FTIR (cm^{-1}) 2930.2, 2867.4, 2851.2, 1732.7, 1624.7, 1603.6, 1576.5, 1507.4, 1466.8, 1376.71, 1250.9, 1172.2, 1033.8, 1016.4, 969.6, 883.6, 842.1, 795.6, 749.3, 606.6, 570.4, 546.5.

Elemental Analysis:

Table S1. The observed C H N % for the final compounds.

Compound	**Molecular Weight**	**Molecular Formula**	**Elemental Analysis (%) Found (Theoretical)**		
			C	**H**	**N**
P-5	4305.07	$C_{276}\ H_{384}\ N_9\ O_{24}\ P_3$	76.54 (77)	9.3 (8.9)	3.2 (2.9)
P-6	4389.23	$C_{282}\ H_{396}\ N_9\ O_{24}\ P_3$	77.1 (77.2)	9.6 (9.1)	2.8 (2.9)
P-7	4473.39	$C_{288}\ H_{408}\ N_9\ O_{24}\ P_3$	76.9 (77.3)	9.5 (9.2)	2.8 (2.8)
P-8	4557.55	$C_{294}\ H_{420}\ N_9\ O_{24}\ P_3$	77.3 (77.5)	9.5 (9.3)	2.8 (2.8)
P-10	4725.88	$C_{306}\ H_{444}\ N_9\ O_{24}\ P_3$	77.3 (77.8)	9.7 (9.5)	2.6 (2.7)
P-11	4810.04	$C_{312}\ H_{456}\ N_9\ O_{24}\ P_3$	77.5 (77.9)	9.7 (9.6)	2.7 (2.6)

NMR spectra of the compounds

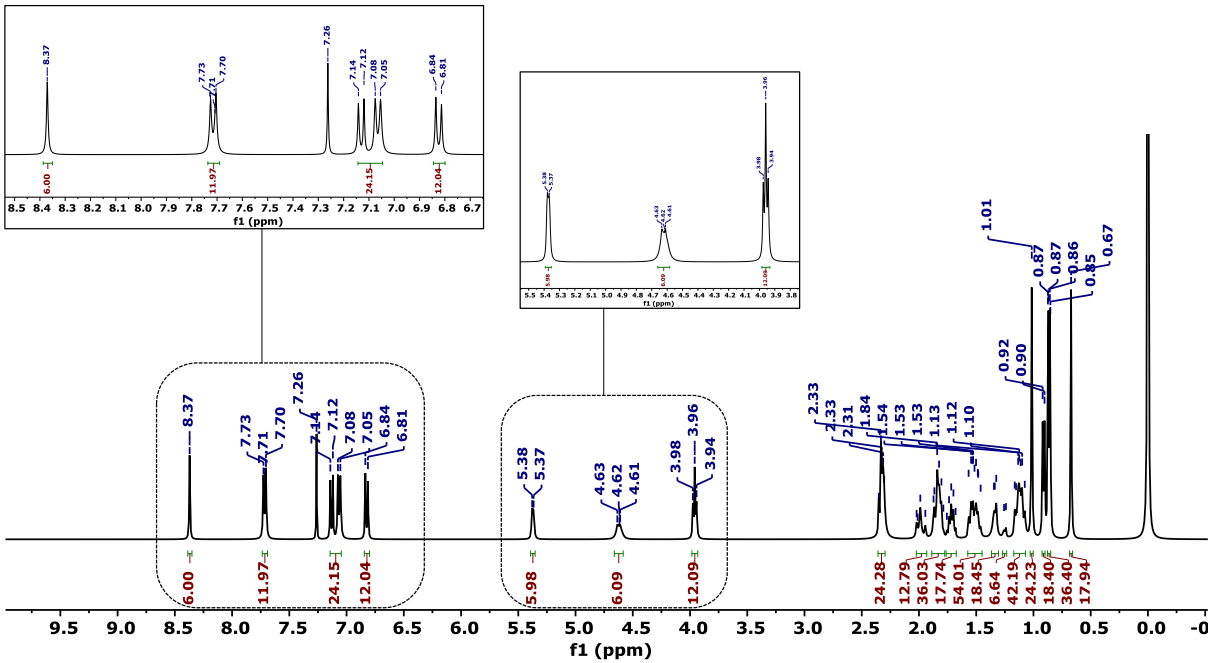

Fig. S4 ^{1}H NMR spectrum of compound **P-5** in $CDCl_3$.

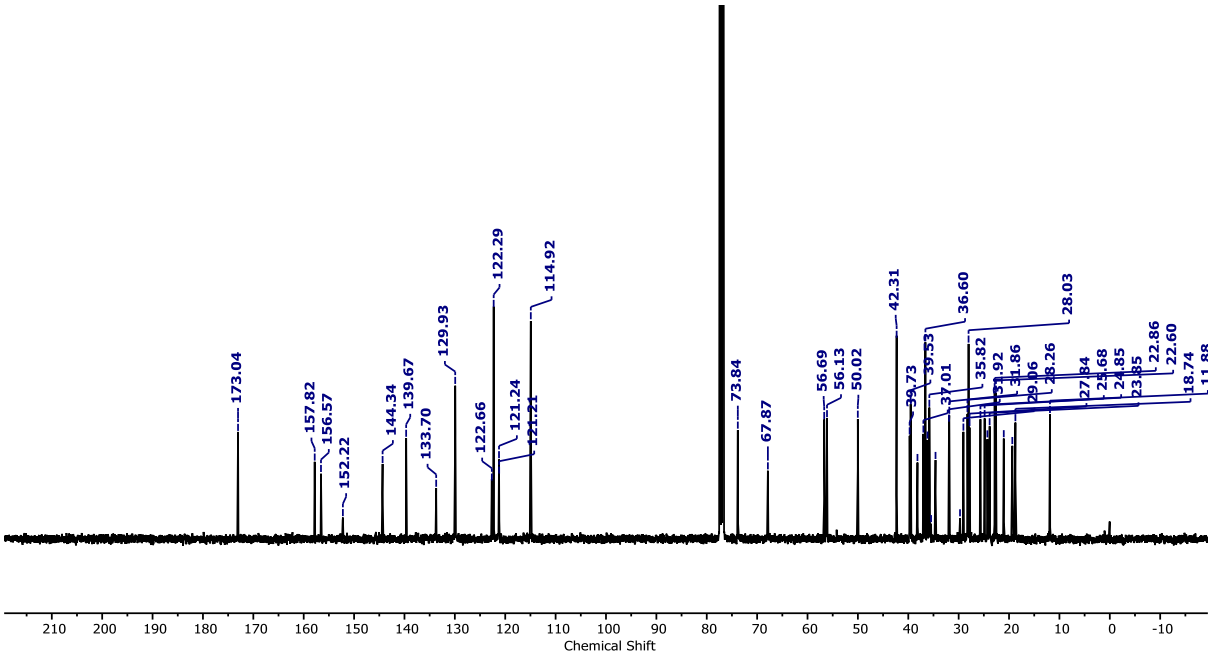

Fig. S5 ^{13}C NMR spectrum of compound **P-5** in $CDCl_3$.

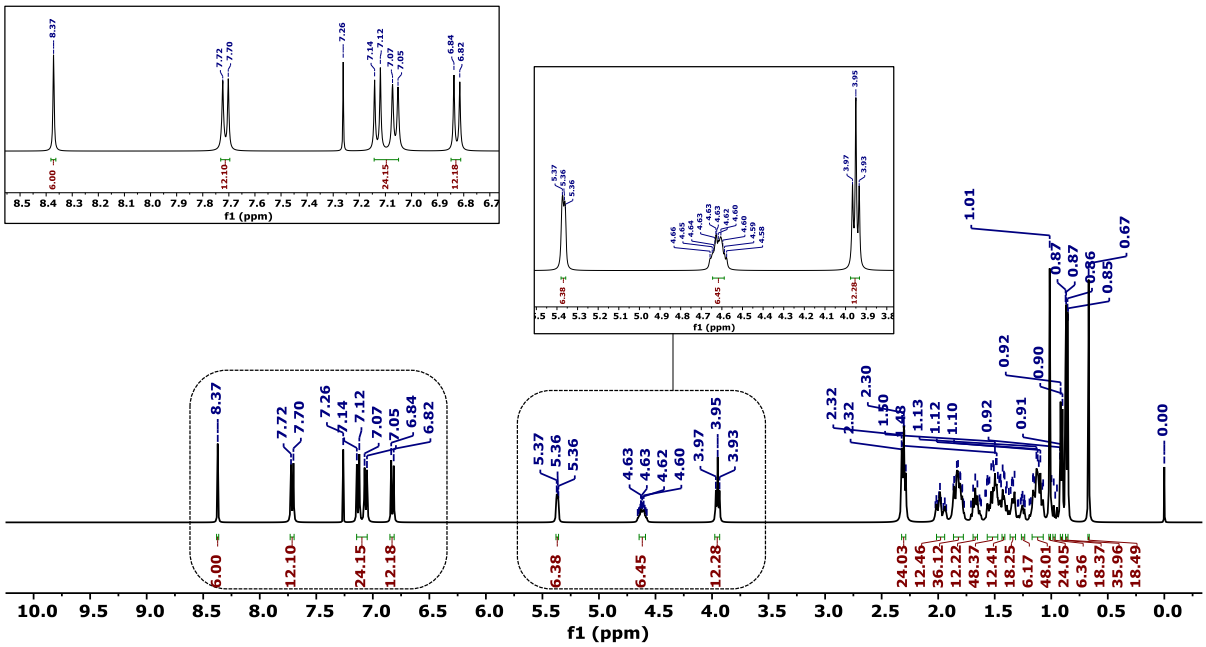

Fig. S6 ^{1}H NMR spectrum of compound **P-6** in $CDCl_3$.

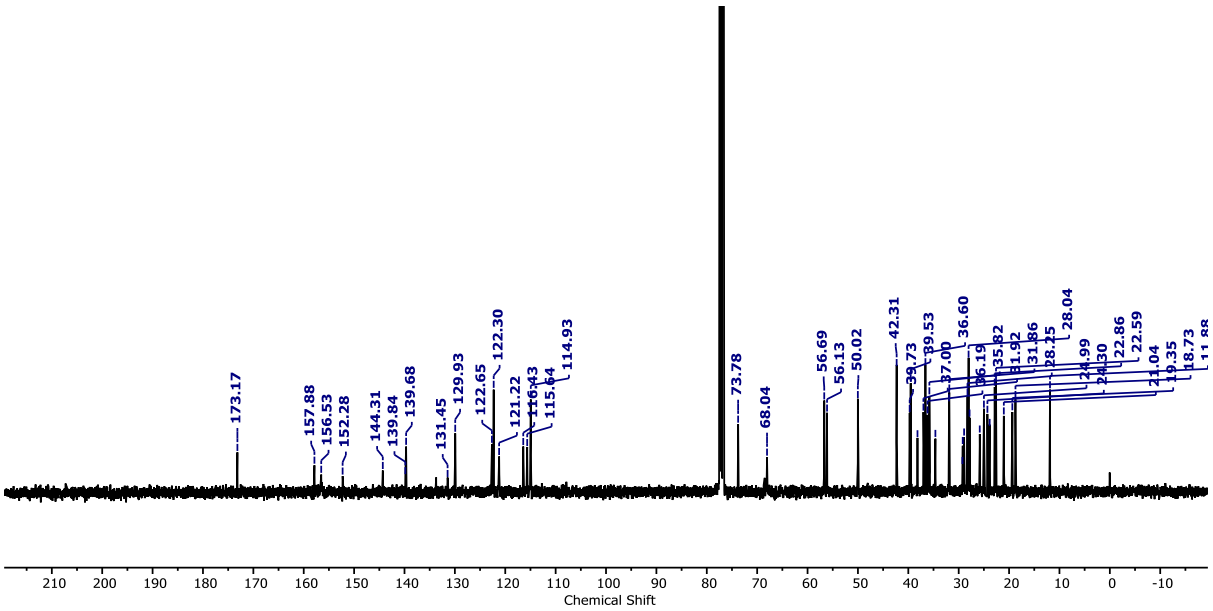

Fig. S7 ^{13}C NMR spectrum of compound **P-6** in $CDCl_3$.

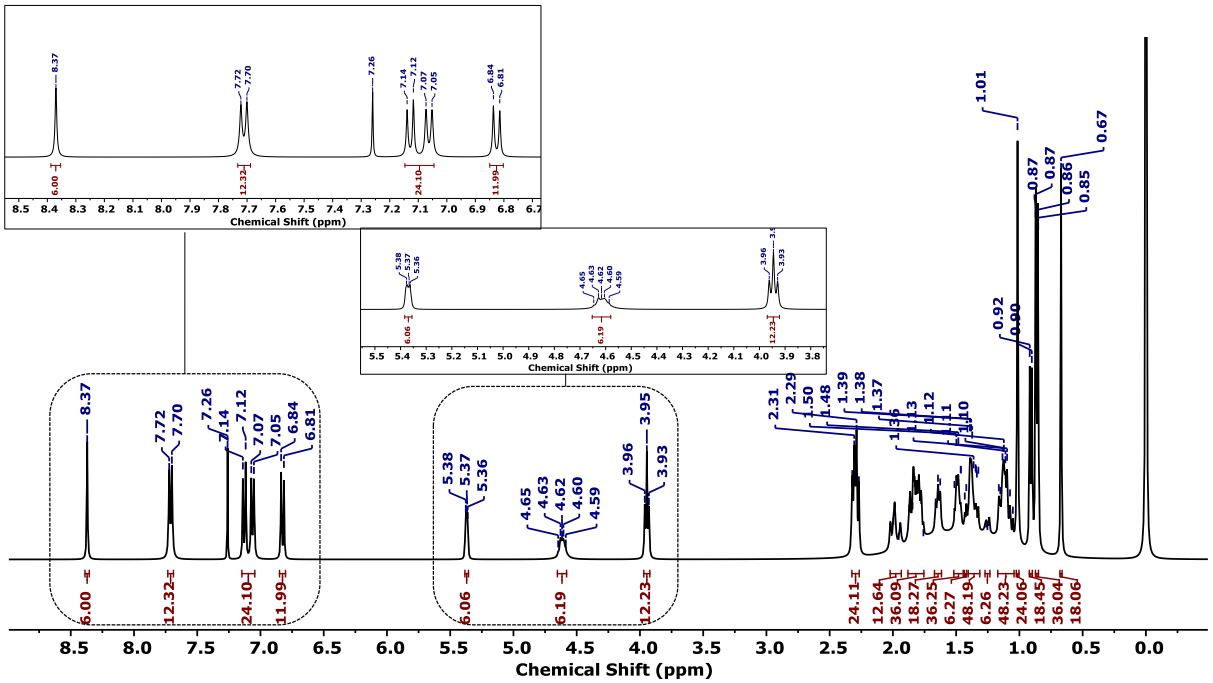

Fig. S8 ^{1}H NMR spectrum of compound **P-7** in $CDCl_3$.

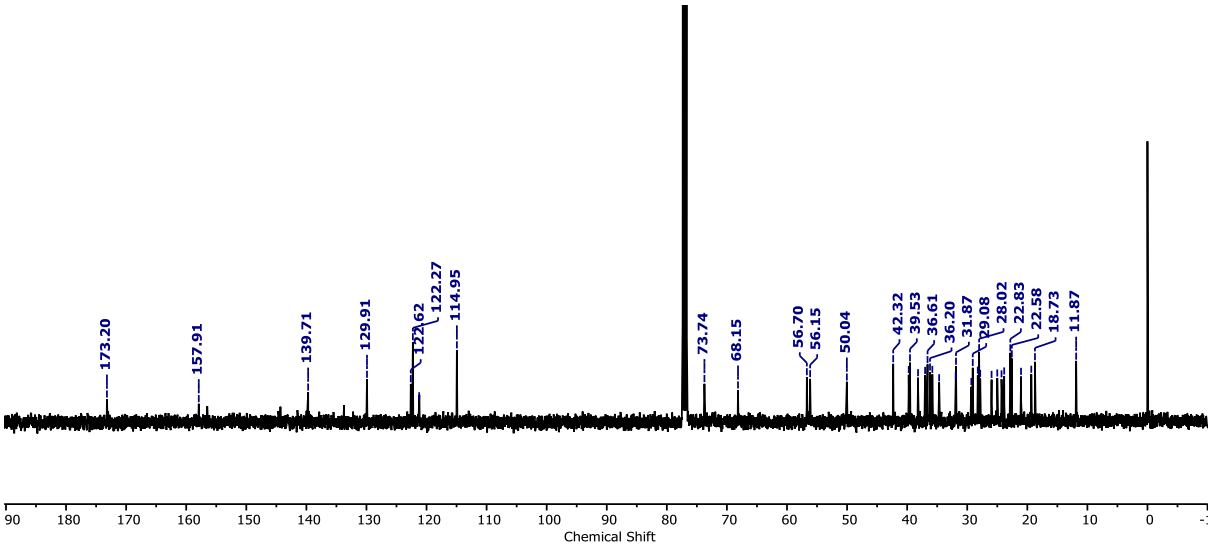

Fig. S9 ^{13}C NMR spectrum of compound **P-7** in $CDCl_3$.

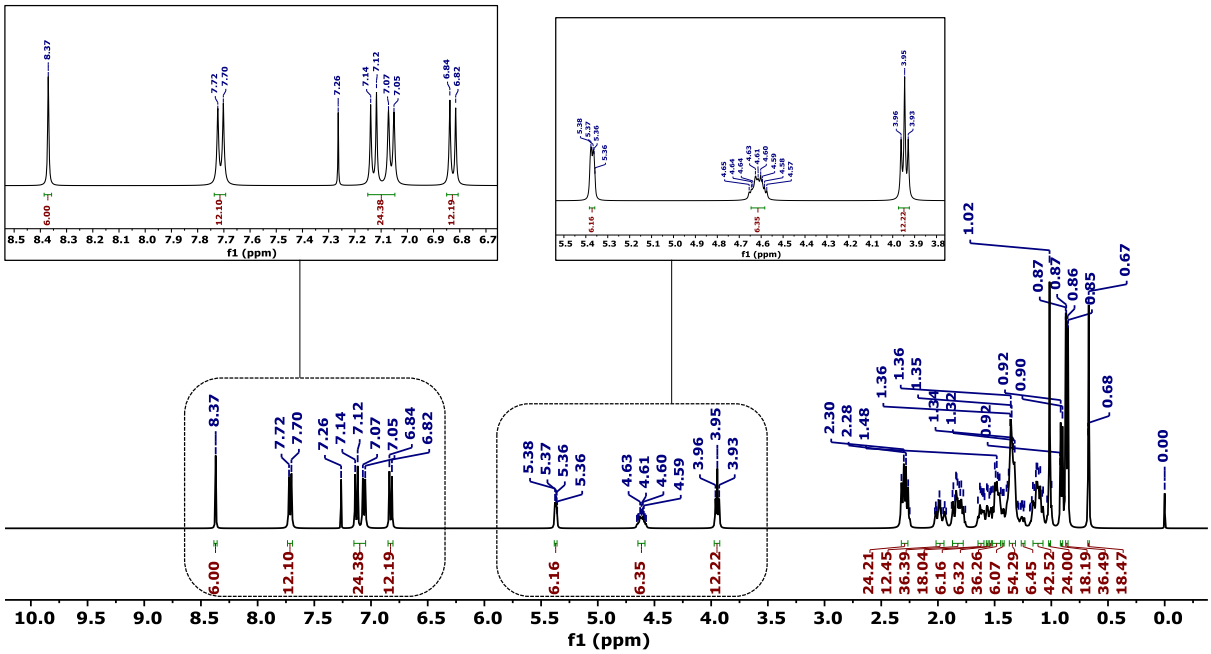

Fig. S10 ^{1}H NMR spectrum of compound **P-8** in $CDCl_3$.

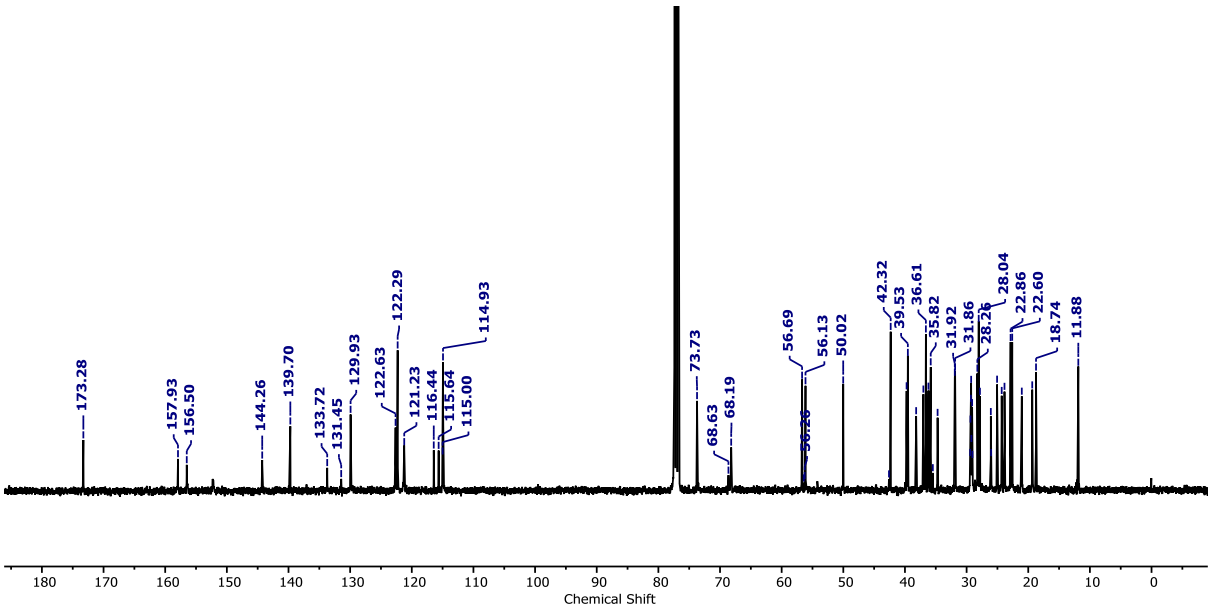

Fig. S11 ^{13}C NMR spectrum of compound **P-8** in $CDCl_3$.

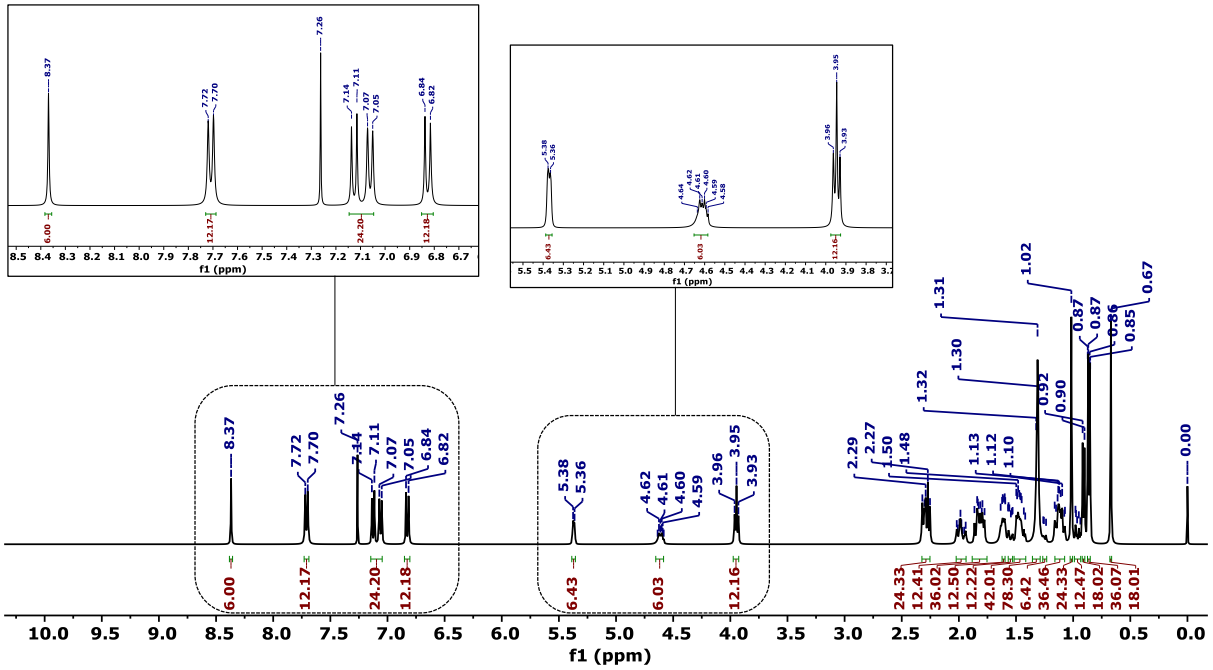

Fig. S12 ^{1}H NMR spectrum of compound **P-10** in $CDCl_3$.

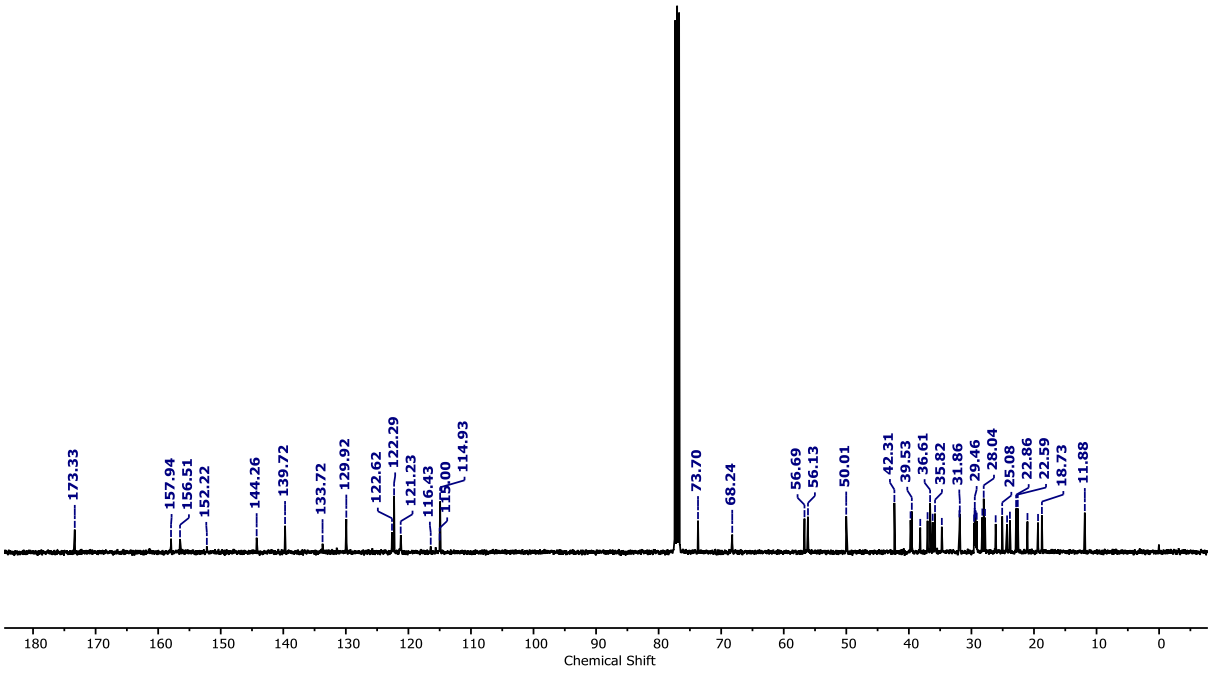

Fig. S13 ^{13}C NMR spectrum of compound **P-10** in $CDCl_3$.

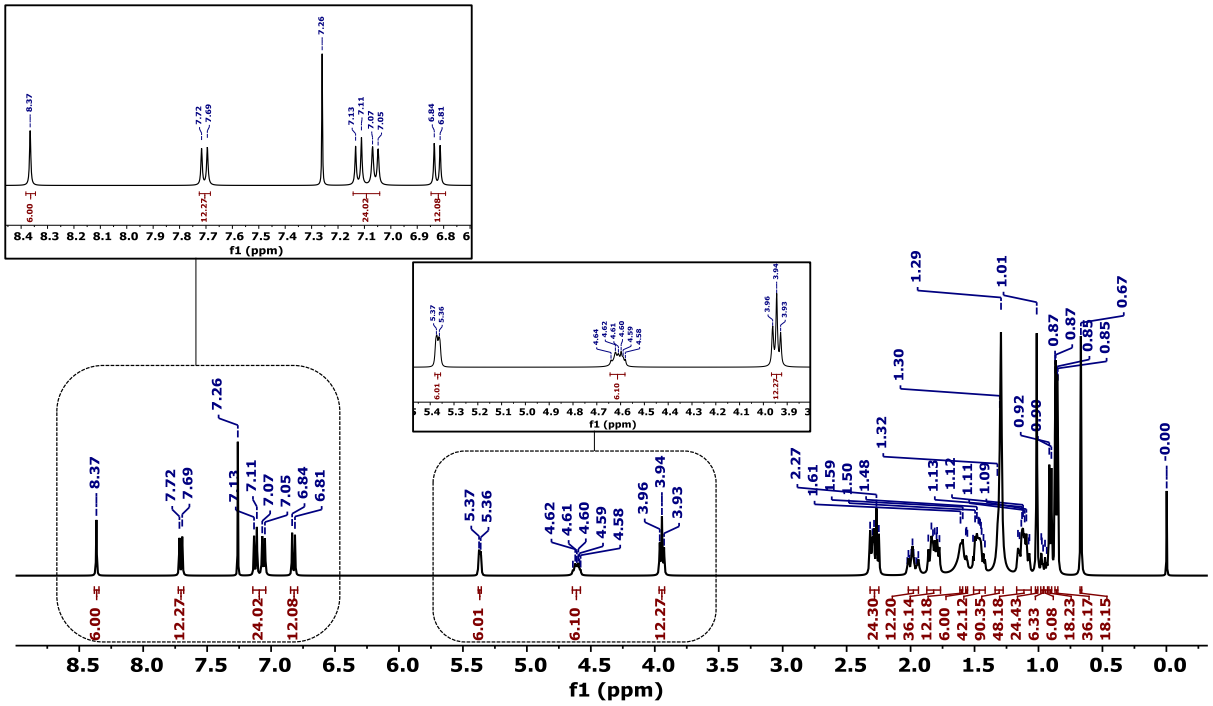

Fig. S14 ^{1}H NMR spectrum of compound **P-11** in $CDCl_3$.

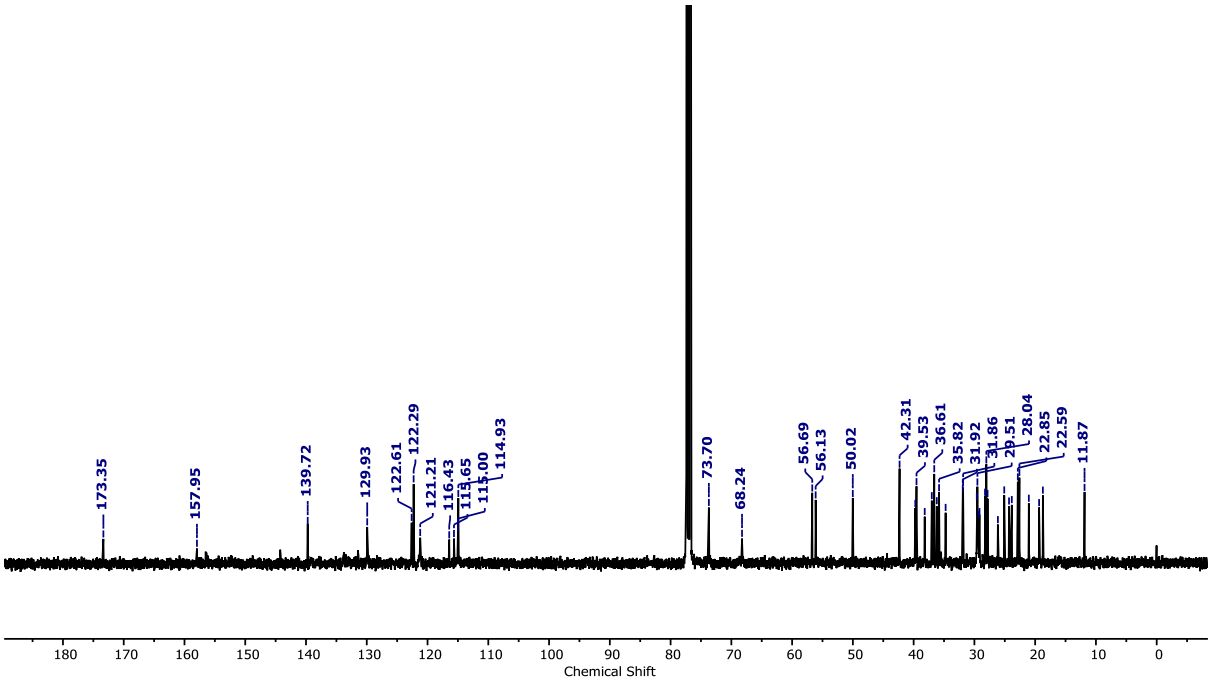

Fig. S15 ^{13}C NMR spectrum of compound **P-11** in $CDCl_3$.

TGA Curves:

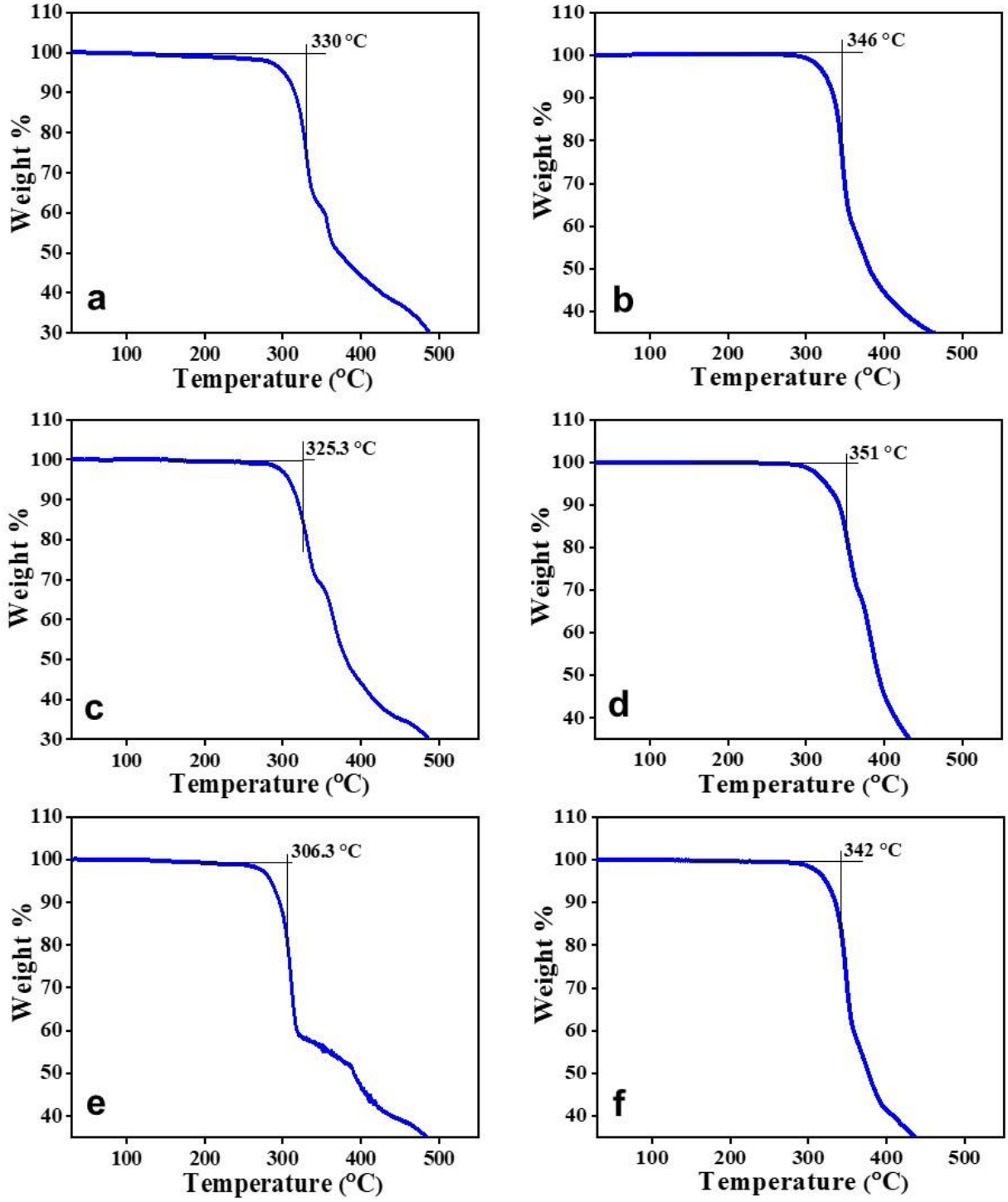

Fig. S16 TGA thermographs of compounds (a) **P-5**, (b) **P-6**, (c) **P-7**, (d) **P-8**, (e) **P-10**, (f) **P-11**, obtained at a rate of 5 °C/min.

DSC Thermograms:

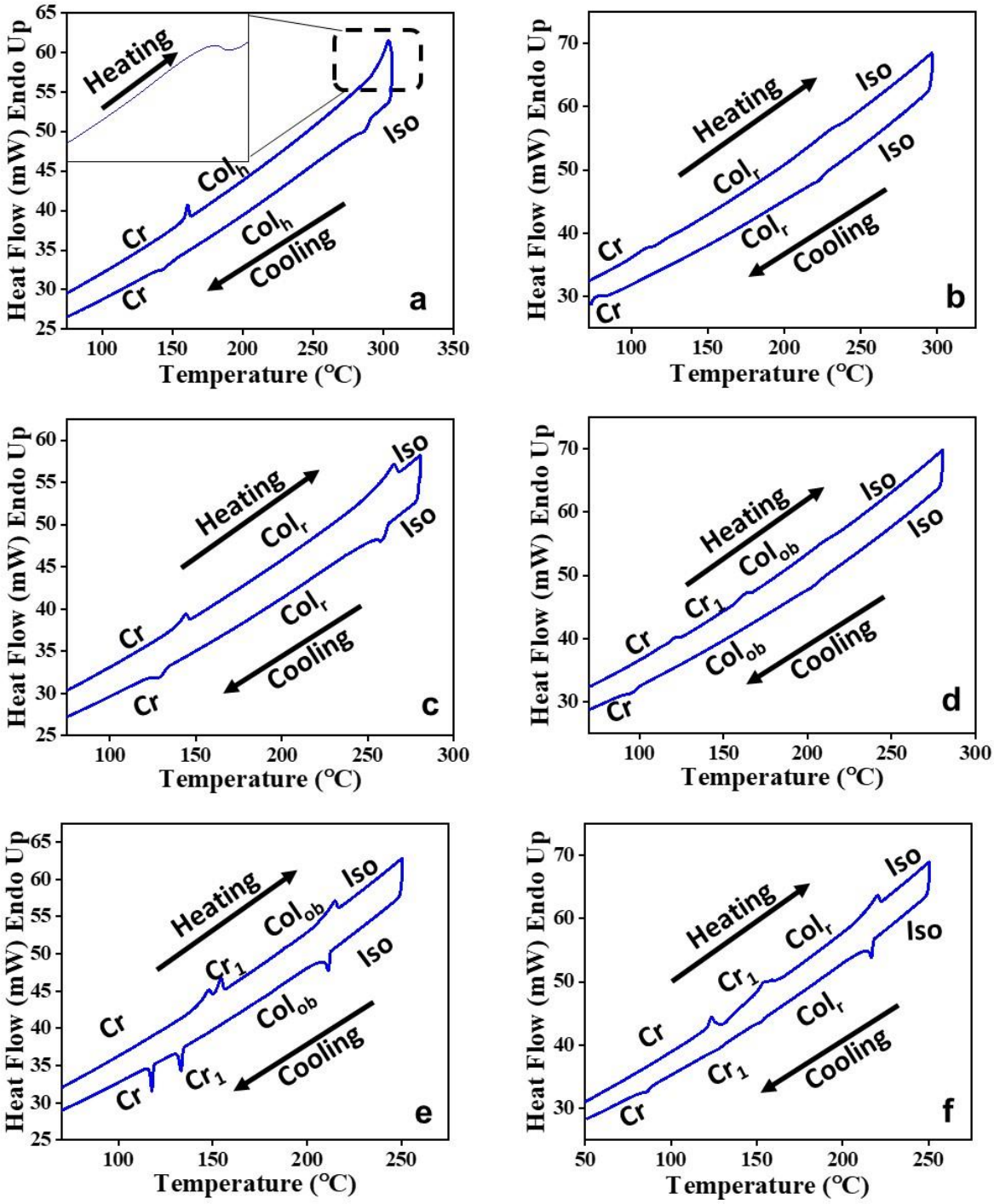

Fig. S17 DSC thermograms of compounds (a) **P-5**, (b) **P-6**, (c) **P-7**, (d) **P-8**, (e) **P-10**, (f) **P-11**, recorded at a rate of 10 °C/min.

X-Ray Diffraction Studies:

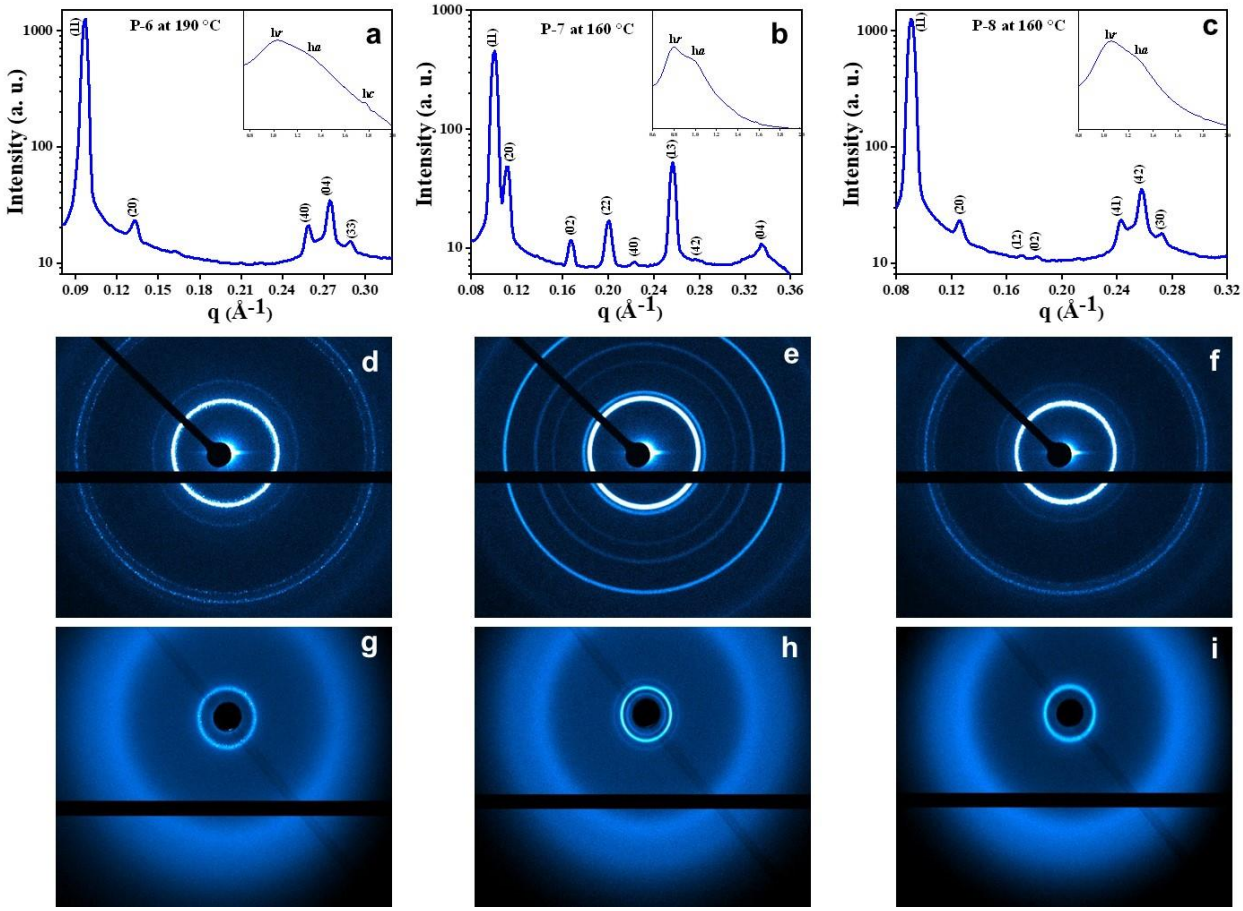

Fig. S18 Small and wide angle (inset) X-ray diffraction patterns of compound (a) **P-6** at 190 °C (Col_r), (b) **P-7** at 160 °C (Col_r) and (c) **P-8** at 160 °C (Col_{ob}) upon cooling, h_r - cholesterol-cholesterol correlation, h_a - alkyl chain-chain correlation. The lower panel shows the respective 2D diffraction patterns of SAXS (d, e, f) and WAXS (g, h, i).

Electron density maps:

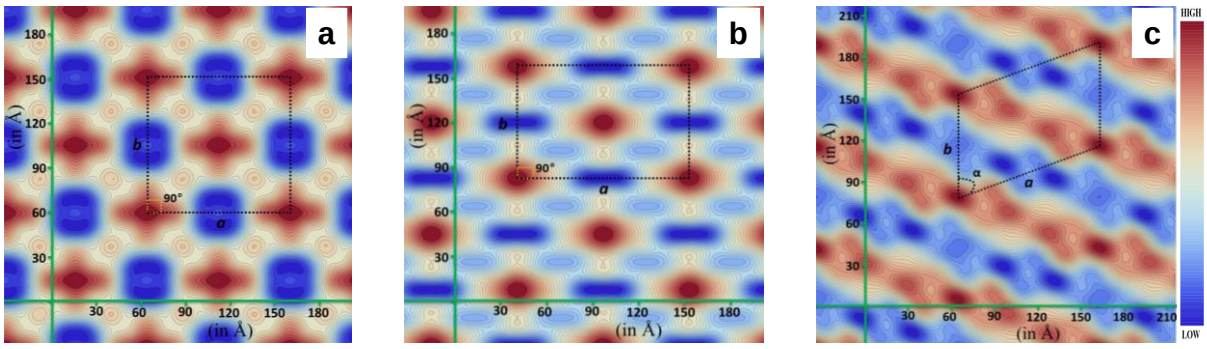

Fig. S19 Electron density map of compound (a) **P-6** in Col_r phase, (b) **P-7** in Col_r phase and (c) **P-8** in Col_{ob} phase. Maroon represents the high electron density region and deep blue is the lowest.

Table S2. The indices observed and calculated *d*-spacings and planes of the diffraction peaks of the hexagonal lattice observed at 160 °C for compound **P-5**. The lattice parameter is a = 72.7 Å. h_r - cholesterol-cholesterol correlation, h_a - alkyl chain-chain correlation. [a] MI: Miller indices. [b]d_{obs}: experimental *d*-spacing. [c]d_{cal}: calculated *d*-spacing by using the relation $\frac{1}{d_{cal}^2} = \frac{4}{3}\left[\frac{h^2+h\,k+k^2}{a^2}\right]$; [d]RI: Relative Intensity. [e]M: Multiplicity.

[a]**MI** (***hk***)	[b]d_{obs} (Å)	[c]d_{cal} (Å)	[d]**RI** (***hk***)	[e]**M**	**Phase Φ (*hk*)**
10	62.9	62.9	100	6	0
11	36.1	36.4	3	6	0
20	31.7	31.5	2	6	0
21	23.7	23.8	8.5	12	л
h_r	6.3				
h_a	5.1				

Table S3. The indices observed and calculated *d*-spacings and planes of the diffraction peaks of the rectangular lattice observed at 190 °C for compound **P-6**. The lattice parameters are a = 96.1 Å, b = 91.1 Å. h_r - cholesterol-cholesterol correlation, h_a - alkyl chain-chain correlation, h_c - disc-disc correlations. [a] MI: Miller indices. [b]d_{obs}: experimental *d*-spacing. [c]d_{cal}: calculated *d*-spacing by using the relation: $\frac{1}{d_{cal}^2} = [\frac{h^2}{a^2} + \frac{k^2}{a^2}]$ [d]RI: Relative Intensity. [e]M: Multiplicity.

[a]**MI** (***hk***)	[b]d_{obs} (Å)	[c]d_{cal} (Å)	[d]**RI** (***hk***)	[e]**M**	**Phase Φ (*hk*)**
11	66.1	66.1	100	4	0
20	48.1	48.1	1.8	2	л
40	24.2	24	1.7	2	0
04	22.9	22.8	2.8	2	0
33	21.8	22.1	1.3	4	л
h_r	6.1				
h_a	5.1				
h_c	3.6				

Table S4. The indices observed and calculated *d*-spacings and planes of the diffraction peaks of the rectangular lattice observed at 160 °C for compound **P-7**. The lattice parameters are a = 112 Å, b = 75.1 Å. h_r - cholesterol-cholesterol correlation, h_a - alkyl chain-chain correlation. [a]MI: Miller indices. [b]d_{obs}: experimental *d*-spacing. [c]d_{cal}: calculated *d*-spacing by using the relation: $\frac{1}{d_{cal}^2} = [\frac{h^2}{a^2} + \frac{k^2}{a^2}]$ [d]RI: Relative Intensity. [e]M: Multiplicity.

[a]**MI** (***hk***)	[b]d_{obs} (Å)	[c]d_{cal} (Å)	[d]**RI** (***hk***)	[e]**M**	**Phase Φ (*hk*)**
11	62.3	62.3	100	4	0
20	56	60	10.6	2	0
02	37.4	37.5	2.6	2	0
22	31.3	31.2	3.8	4	л
40	28.1	28	1.7	2	0
13	24.5	24.4	11.5	4	0
42	22.5	22.4			//
04	18.8	18.8	2.4	2	л
h_r	6.1				
h_a	5				

Table S5. The indices observed and calculated *d*-spacings and planes of the diffraction peaks of the oblique lattice observed at 160 °C for compound **P-8**. The lattice parameters are a = 105.2 Å, b = 73.7 Å and α = 69.3°. h_r - cholesterol-cholesterol correlation, h_a - alkyl chain-chain correlation. [a]MI: Miller indices. [b]d_{obs}: experimental *d*-spacing. [c]d_{cal}: calculated *d*-spacing by using the relation: $\frac{1}{d_{cal}^2} = \frac{1}{Sin^2\alpha}\left[\frac{h^2}{a^2} + \frac{k^2}{b^2} - \frac{2\,h\,k\,Cos\alpha}{a\,b}\right]$; [d]RI: Relative Intensity. [e]M: Multiplicity.

[a]**MI** (***hk***)	[b]d_{obs} (Å)	[c]d_{cal} (Å)	[d]**RI** (***hk***)	[e]**M**	**Phase Φ (*hk*)**
11	69.2	69.1	100	2	0
20	49.5	49.2	1.8	2	л
12	36.9	36.9	0.9	2	0
02	34.5	34.5	0.9	2	0
41	26	26.3	1.9	2	0
42	24.6	24.6	3.4	2	0
03	23.1	22.9	1.4	2	0
h_r	6.1				
h_a	4.9				

Table S6. The indices observed and calculated *d*-spacings and planes of the diffraction peaks of the oblique lattice observed at 160 °C for compound **P-10**. The lattice parameters are a = 106.7 Å, b = 78.5 Å and α = 79.6°. h_r - cholesterol-cholesterol correlation, h_a - alkyl chain-chain correlation. [a]MI: Miller indices. [b]d_{obs}: experimental *d*-spacing. [c]d_{cal}: calculated *d*-spacing by using the relation: $\frac{1}{d_{cal}^2} = \frac{1}{Sin^2\alpha}\left[\frac{h^2}{a^2} + \frac{k^2}{b^2} - \frac{2\,h\,k\,Cos\alpha}{a\,b}\right]$; [d]RI: Relative Intensity. [e]M: Multiplicity.

[a]**MI** (***hk***)	[b]d_{obs} **(Å)**	[c]d_{cal} **(Å)**	[d]**RI** (***hk***)	[e]**M**	**Phase Φ (*hk*)**
11	68.4	68.4	100	2	0
20	52.4	52.5	8.2	2	0
21	47.5	47.6	2.8	2	0
12	38.6	38.6	3	2	0
22	34.6	34.2	3	2	0
40	26.5	26.2	19.5	2	0
24	19.6	19.3	2.3	2	л
h_r	6.1				
h_a	4.9				

Table S7. The indices observed and calculated *d*-spacings and planes of the diffraction peaks of the rectangular lattice observed at 180 °C for compound **P-11**. The lattice parameters are a = 148.2 Å, b = 79.9 Å. h_r - cholesterol-cholesterol correlation, h_a - alkyl chain-chain correlation, h_c - disc-disc correlations. [a]MI: Miller indices. [b]d_{obs}: experimental *d*-spacing. [c]d_{cal}: calculated *d*-spacing by using the relation: $\frac{1}{d_{cal}^2} = \left[\frac{h^2}{a^2} + \frac{k^2}{a^2}\right]$; [d]RI: Relative Intensity. [e]M: Multiplicity.

[a]**MI** (***hk***)	[b]d_{obs} **(Å)**	[c]d_{cal} **(Å)**	[d]**RI** (***hk***)	[e]**M**	**Phase Φ (*hk*)**
11	70.3	70.3	100	4	л
02	40	39.9	8.2	2	л
51	27.9	27.8	28.9	4	л
62	20.8	21	4.3	4	л
h_r	6.1				
h_a	5.2				
h_c	3.6				

UV-visible data:

The photophysical behaviour of phosphazene based mesogens has been investigated by UV-vis spectroscopy. The absorption spectra have been recorded in the 10^{-5} M THF solution for all the compounds at room temperature as shown in Fig S20(a-f). All the compounds show a strong absorption band around 273 nm, which corresponds to π-π* transition due to phosphazene and benzene, and a lower peak around 338 nm, which indicates the n-π* transition due to nitrogen and oxygen atoms of the molecule.[6] The fluorescence spectra have also been recorded in the 10^{-5} M THF (λ_{max} = 338 nm) solution for all the compounds at room temperature, as shown in Fig. S21(a-f).

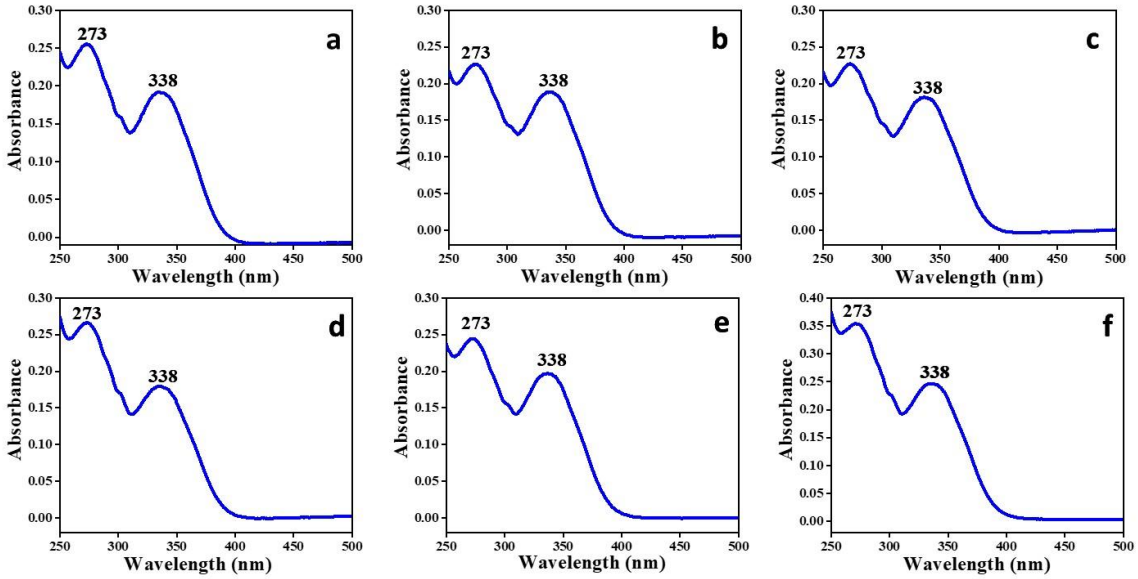

Fig. S20 Absorption spectra of compounds (a) **P-5**, (b) **P-6**, (c) **P-7**, (d) **P-8**, (e) **P-10**, (f) **P-11**, in 10^{-5} M THF solution.

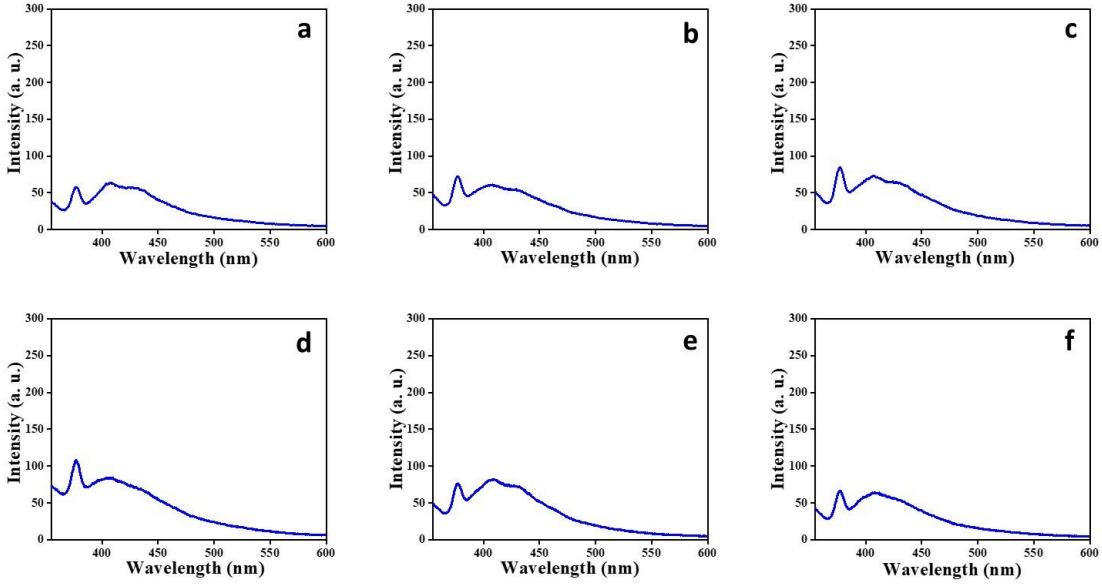

Fig. S21 Emission spectra of compounds (a) **P-5**, (b) **P-6**, (c) **P-7**, (d) **P-8**, (e) **P-10**, (f) **P-11**, in 10^{-5} M THF solution, where the excitation wavelength is 338 nm.

Circular Dichroism (CD) Spectroscopy:

Chiroptical measurements:

The requisite sample cells (thin-films) were fabricated by using two clean, regular quartz plates. About 500-800 µg of the samples, **P-6**, **P-10** and **P-11**, placed individually between the substrates, were heated to their isotropic state, and the top plate was hard-pressed repeatedly to attain the uniform spreading of the analyte over a large area of the cell. This procedure not only expels the air-pockets but also ensures the thin-film formation of the mesogens. Although an analyte cell was fabricated for the study using a tiny amount (~600 µg) of mesogen **P-5**, the aforesaid protocol could not be adopted due to its high isotropization temperature. The fabrication of such ultra thin-films, using a minute amount of the samples, was essential to circumvent the factual errors associated with experiments and operating limits of the instrument. The samples were then cooled at a faster rate into the LC phase, and the CD spectra were recorded as a function of decreasing temperature. Tables S8, S9, S10 and S11 respectively portray the CD data, presented in terms of ellipticity (θ, in millidegrees, mdeg) as a function of wavelength, derived from the temperature-dependent CD profiles of the mesogens **P-5** (Fig. S22b), **P-6** (Fig. 6g) **P-10** (Fig. 6h), and **P-11** (Fig. 6i). As noted earlier, CD spectra are often affected by the LD artifacts resulting from the macroscopic optical anisotropies of the analyte. Thus, to differentiate the specimens' genuine CD activity from that of the spurious response, the LD spectra were recorded using the instrument's built-in LD data acquisition option. This observation was corroborated using the sample rotation technique, which is very useful and reliable for the thin, evenly spread anisotropic samples. The CD spectra were recorded at six different positions attained by step-wise 60° rotation of the cell in the observing plane, i.e., in the direction perpendicular to the measuring beam. As expected, the CD profiles recorded for different cells' orientations largely resembled each other implying the absence of the LD. The spectra recorded did not show any signatures due to LD activity (Fig. S22a), as contemplated.

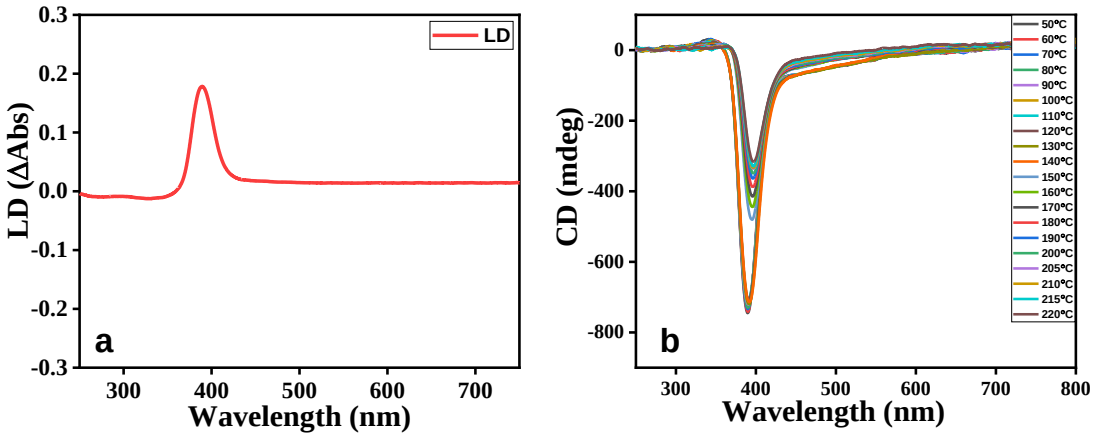

Fig. S22 (a) The LD spectrum of the fluid Col phase of compound **P-5,** (b) CD spectra were obtained as a function of temperature for the Col phase of compound **P-5**. It may be noted here that the CD intensity increases with the decrease in temperature of the Col phase.

Table S8. CD spectral data of the Col phase exhibited by the compound **P-5**.

Temperature (°C)	CD	
	λ_{max} / nm	CD (mdeg)
50	390	-744
60	390	-742
70	390	-740
75	390	-738
80	390	-736
90	390	-734
100	390	-732
110	390	-730
120	390	-728
130	390	-726
140	390	-725
150	390	-479
160	393	-436
170	393	-409
180	393	-375
190	395	-357
200	395	-339
210	395	-332
215	395	-324
220	396	-313

Table S9. CD spectral data of the Col phase exhibited by the compound **P-6**.

Temperature (°C)	CD	
	λ_{max} / nm	CD (mdeg)
55	360, 297	-947, -270
60	360, 297	-942, -270
70	360, 297	-940, -269
75	360, 297	-938, -269
80	360, 297	-913, -264
90	360, 297	-880, -259
100	360, 297	-875, -254
110	360, 297	-853, 249
120	360, 297	-819, -245
130	360, 297	-700, -231
140	400, 350	-198, -134
150	400, 350	-197, -90
160	400, 350	-194, 58

170	400, 350	-188, -35
180	400, 350	-175, -25
190	400	-170
200	400	-168
210	400	-168
220	400	-167

Table S10. CD spectral data of the Col phase exhibited by the compound **P-10**.

Temperature (°C)	CD	
	λ_{max} / nm	CD (mdeg)
70	393	-100
80	393	-95
90	398	-73
100	399	-65
110	398	-58
120	398	-57
130	397	-56
140	397	-56
150	398	-55
160	398	-45
170	398	-40
180	398	-37
190	399	-34
200	399	-33

Table S11. CD spectral data of the Col phase exhibited by the compound **P-11**.

Temperature (°C)	CD	
	λ_{max} / nm	CD (mdeg)
90	385	-153
100	385	-144
110	385	-143
120	385	-140
130	387	-132
140	387	-130
150	388	-82
160	388	-74
170	388	-71
180	390	-61

HCl Sensing:

For the sensing experiments, stock solutions of compound **P-11** and HCl were prepared. In particular, 10^{-5} M solution of compound **P-11** in THF and 10^{-2} M HCl solution in ACN were prepared. Titration experiments were performed by adding HCl solution at a gradual interval of 10 μL to the stock solution of compound **P-11**, where the excitation wavelength is 338 nm. The fluorescence spectra were recorded accordingly with excitation and emission slit widths of 5.0 nm. Similarly, the selectivity experiments were carried out by adding 50 μL of 0.1 M stock solution of various acids in 600 μL stock solution of compound **P-11**. The detection limit (LOD) was calculated using the formula $3\sigma/\rho$, where σ is the standard deviation of blank measurements of compound **P-11** and ρ is the slope of the calibration curve plotted between fluorescence intensity and HCl concentration. The optical photographs of the compounds **P-5**, **P-6**, **P-7**, **P-8**, and **P-10** displayed the similar behaviour towards HCl vapour are shown in Fig. S23-S27 below.

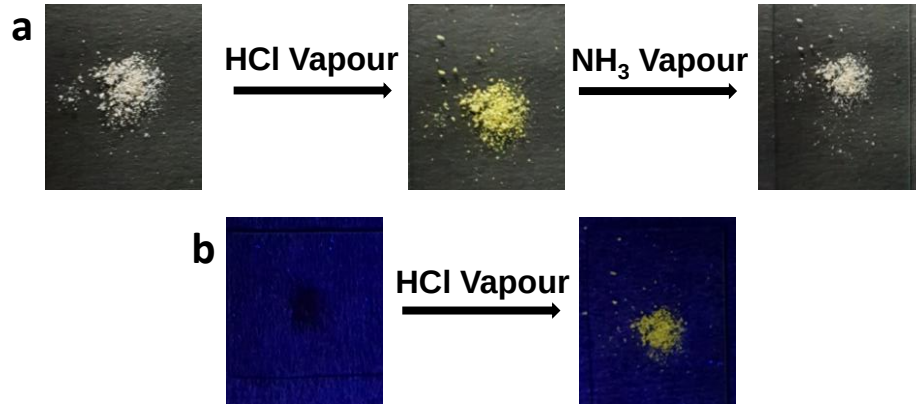

Fig. S23 Optical photographs of **P-5**, **(a)** upon exposure to HCl vapor and ammonia vapor under normal light, and **(b)** upon exposure to HCl vapor under UV light.

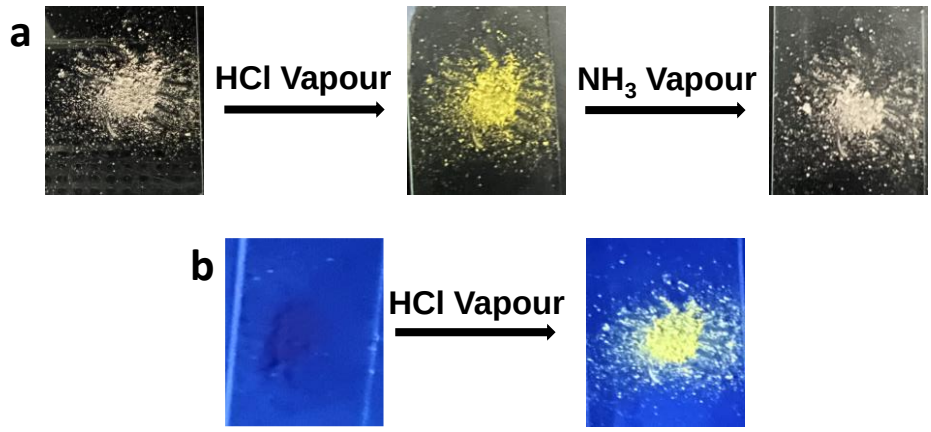

Fig. S24 Optical photographs of **P-6**, **(a)** upon exposure to HCl vapor and ammonia vapor under normal light, and **(b)** upon exposure to HCl vapor under UV light.

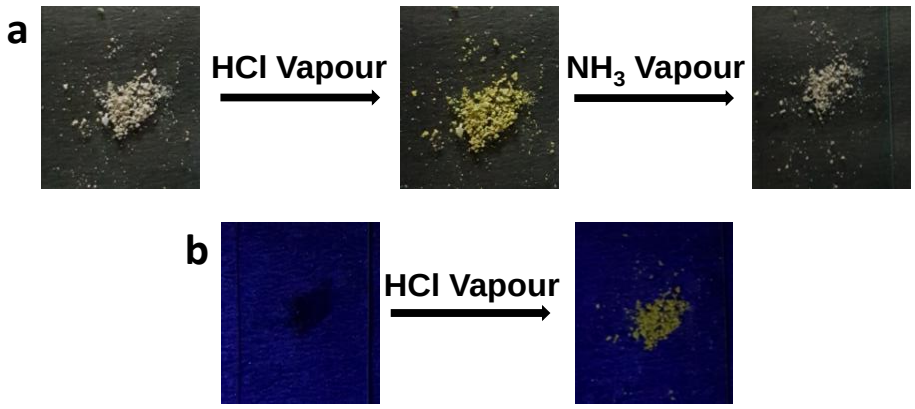

Fig. S25 Optical photographs of **P-7**, **(a)** upon exposure to HCl vapor and ammonia vapor under normal light, and **(b)** upon exposure to HCl vapor under UV light.

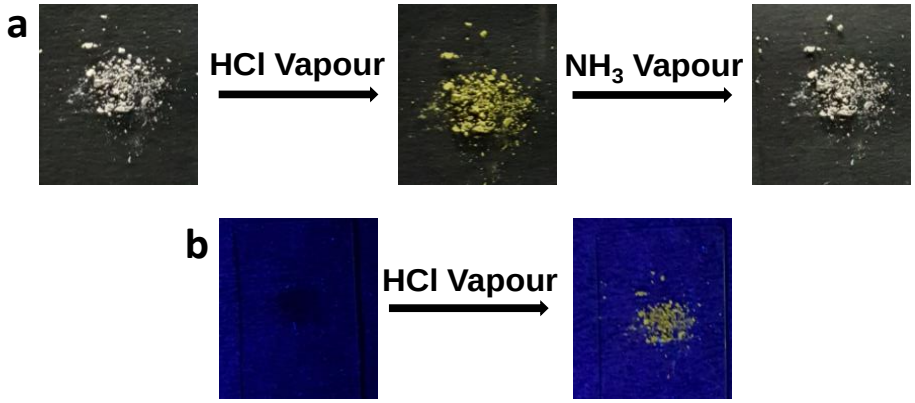

Fig. S26 Optical photographs of **P-8**, **(a)** upon exposure to HCl vapor and ammonia vapor under normal light, and **(b)** upon exposure to HCl vapor under UV light.

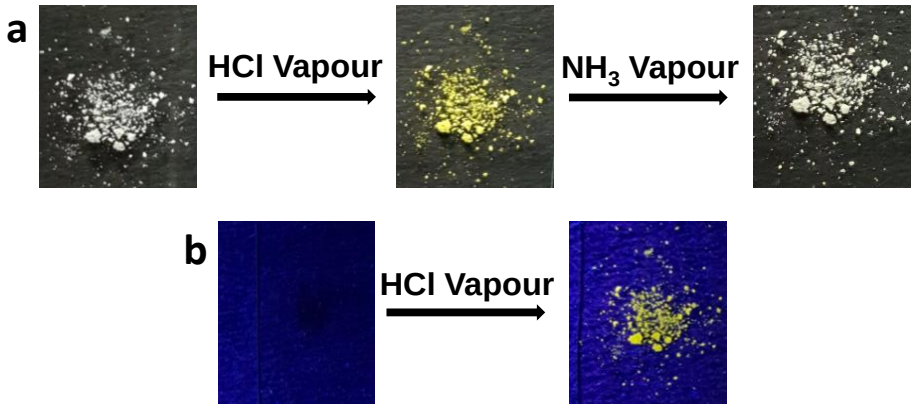

Fig. S27 Optical photographs of **P-10**, **(a)** upon exposure to HCl vapor and ammonia vapor under normal light, and **(b)** upon exposure to HCl vapor under UV light.

References

1. I. Bala, W. Y. Yang, S. P. Gupta, J. De, R. A. K. Yadav, D. P. Singh, D. K. Dubey, J.-H. Jou, R. Douali and S. K. Pal, *J. Mater. Chem. C*, 2019, **7**, 5724-5738.
2. I. Bala, S. P. Gupta, S. Kumar, H. Singh, J. De, N. Sharma, K. Kailasam and S. K. Pal, *Soft matter*, 2018, **14**, 6342-6352.
3. J. De, S. P. Gupta, S. S. Swayamprabha, D. K. Dubey, I. Bala, I. Sarkar, G. Dey, J.-H. Jou, S. Ghosh and S. K. Pal, *J. Phys. Chem. C*, 2018, **122**, 23659-23674.
4. I. Bala, S. P. Gupta, J. De and S. K. Pal, *Chem. Eur. J.*, 2017, **23**, 12767-12778.
5. S. A. Bhat, D. S. S. Rao, S. K. Prasad and C. V. Yelamaggad, *Nanoscale Adv.*, 2021, **3**, 2269–2279.
6. S. M. Örüm and Y. S. Demircioğlu, *Macromol. Res.*, 2018, **26**, 671-679.